Biochem. J. (2012) **441**, 719–730 (Printed in Great Britain) doi:10.1042/BJ20111130

online data

SUPPLEMENTARY ONLINE DATA

Regulation by mitochondrial superoxide and NADPH oxidase of cellular formation of nitrated cyclic GMP: potential implications for ROS signalling

Khandaker Ahtesham AHMED*, Tomohiro SAWA*†, Hideshi IHARA‡, Shingo KASAMATSU‡, Jun YOSHITAKE*, Md. Mizanur RAHAMAN*, Tatsuya OKAMOTO*, Shigemoto FUJII* and Takaaki AKAIKE*[1]

*Department of Microbiology, Graduate School of Medical Sciences, Kumamoto University, 1-1-1 Honjo, Kumamoto 860-8556, Japan, †PRESTO, Japan Science and Technology Agency (JST), 4-1-8 Honcho Kawaguchi, Saitama 332-001, Japan, and ‡Department of Biological Science, Graduate School of Science, Osaka Prefecture University, 1-1 Gakuen-cho, Sakai, Osaka 599-8531, Japan

MATERIALS AND METHODS

MitoTracker® Green staining

In order to confirm the mitochondrial origin of superoxide generated by LPS/cytokine stimulation, we performed double staining of cells with 50 nM MitoTracker® Green FM dissolved in Hank's buffer [1] (excitation at 488 nm; green photomultiplier channel of the confocal microscope used for image acquisition) plus 2.5 μM MitoSOX™ Red dissolved in Hank's buffer, for 15 min.

Nitrite and nitrate measurement

C6 cells were seeded in a 96-well plate at a density of 10^5 cells/well, followed by stimulated with LPS/cytokines in the absence or the presence of PEG–SOD (200 units/ml) or PEG–catalase (200 units/ml) for 36 h. We quantified NO_2^- and NO_3^- produced in C6 cells using an HPLC-flow reactor system, as described previously [2].

Superoxide and H_2O_2 measurements

C6 cells were seeded in 12-well plate at a density of 2×10^5 cells/well, followed by treated with control siRNA or $p47^{phox}$ siRNA, or untreated for 36 h. Cells were then stimulated with LPS/cytokines for a further 36 h. Cells were then washed twice with PBS, followed by measurement of superoxide and H_2O_2. Superoxide production by C6 cells was measured by means of cytochrome *c* reduction assay, as described previously [3]. Cytochrome *c* reduction was measured by reading the absorbance at 550 nm. Superoxide production was calculated from SOD-inhibitable absorbance using coefficient for change of ferricytochrome *c* to ferrocytochrome *c* (i.e. 21.0 mmol/l per cm). For H_2O_2 measurement, C6 cells was incubated in PBS at 37 °C for 10 min, and H_2O_2 produced in the supernatant was measured by using a hydrogen peroxide colorimetric detection kit (Enzo Life Sciences, catalogue number ADI-907-015) according to the manufacturer's protocol.

Cell viability assay

C6 cells were seeded in a 96-well plate at a density of 10^3 cells/well, followed by stimulation with LPS/cytokines in the presence of tiron (0, 10 or 100 μM) for 36 h. Cell viability was measured using the Cell Counting Kit-8 (Dojindo Laboratories) according to the manufacturer's protocol.

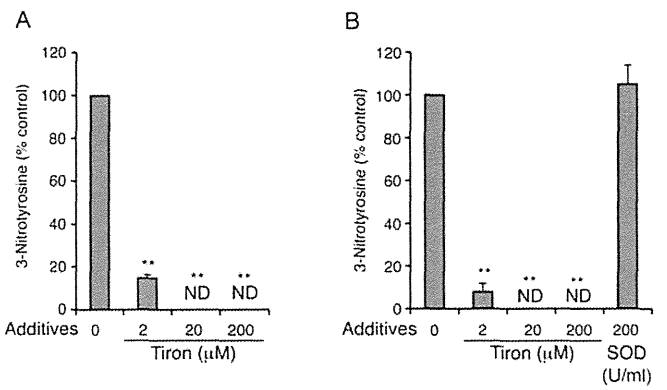

Figure S1 Effect of tiron on tyrosine nitration caused by RNOS

Tyrosine (100 mM) was reacted with $ONOO^-$ (5 mM) (**A**) or with P-NONOate (100 mM) (**B**) in 0.1 M sodium phosphate buffer (pH 7.4) containing 0.1 mM DTPA in the presence of the indicated concentrations of tiron. In (**B**), the effect of SOD (200 units/ml) was also examined. Formation of 3-nitrotyrosine was determined by HPLC-ECD. Data are expressed as means ± S.E.M. ($n = 3$). $^{**}P < 0.01$ compared with the control (without tiron). ND, not detected.

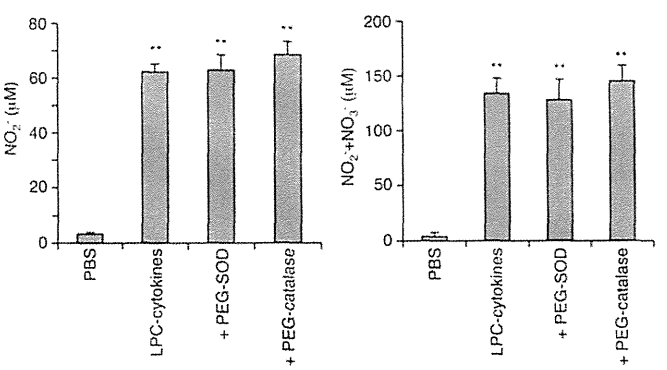

Figure S2 Effect of PEG–SOD and PEG–catalase on NO production from C6 cells

C6 cells were seeded in a 96-well plate at a density of 10^5 cells/well, followed by stimulation with LPS plus pro-inflammatory cytokines in the presence of PEG–SOD (200 units/ml) or PEG–catalase (200 units/ml) for 36 h. NO metabolites (NO_2^- and NO_3^-) in culture supernatants were determined using the Griess assay. Data are expressed as means ± S.E.M. ($n = 3$). $^{**}P < 0.01$ compared with the control (PBS).

[1] To whom correspondence should be addressed (email takakaik@gpo.kumamoto-u.ac.jp).

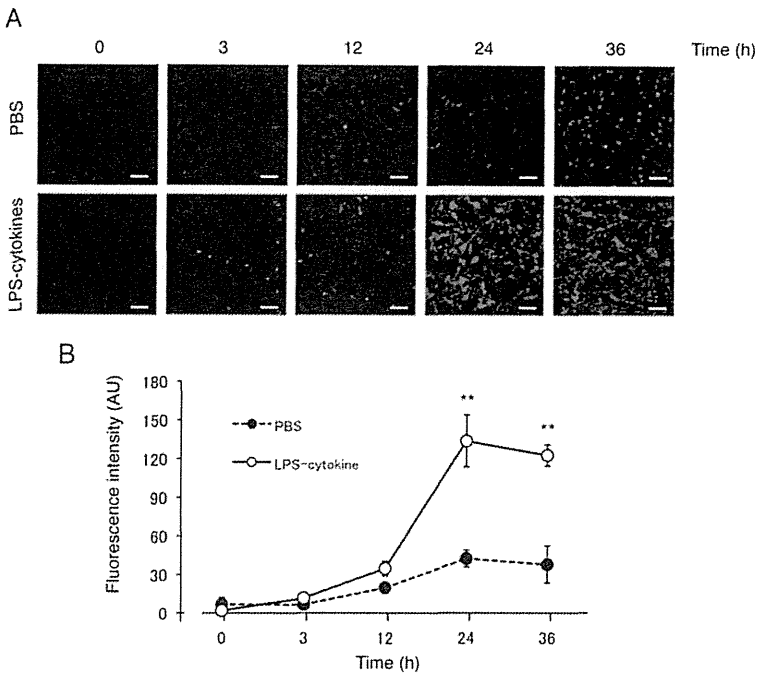

Figure S3 Time-dependent increase in mitochondrial superoxide in rat C6 glioma cells stimulated with LPS/cytokines

Cells were stimulated with a mixture of LPS (10 μg/ml), IFN-γ (200 units/ml), TNF-α (500 units/ml) and IL-1β (10 ng/ml) for 0, 3, 12, 24 and 36 h. Cells were then analysed for the presence of mitochondrial superoxide as described in the Materials and methods section of the main paper. (**A**) MitoSOX™ Red staining of PBS-treated cells (top panels) and LPS/cytokine-treated cells (bottom panels) as detected using a Nikon EZ-C1 confocal laser microscope (for MitoSOX™ Red: excitation at 420 nm and red photomultiplier channel; for DCDHF-DA: excitation at 488 nm and green photomultiplier channel). Scale bars = 50 μm. (**B**) Fluorescence intensity for MitoSOX™ Red staining. Data are expressed as means ± S.E.M. ($n = 3$). $^{**}P < 0.01$ compared with PBS-treated cells.

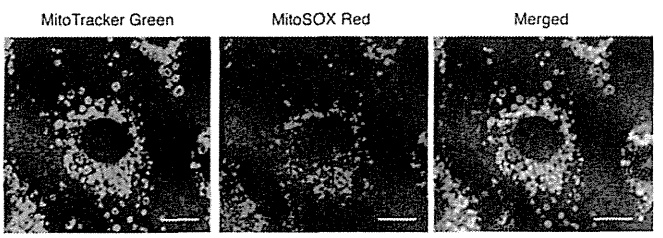

Figure S4 LPS/cytokine stimulation of rat C6 glioma cells produced mitochondrial superoxide

Cells were stimulated with a mixture of LPS (10 μg/ml), IFN-γ (200 units/ml), TNF-α (500 units/ml) and IL-1β (10 ng/ml) for 36 h. Stimulated cells were then analysed for co-localization of mitochondria and superoxide generated in the cells, as described in the Materials and methods section of the supplementary material. MitoTracker® Green (left-hand panel) and MitoSOX™ Red (middle panel) staining of stimulated cells, as detected by the Nikon EZ-C1 confocal laser microscope (for MitoTracker® Green: excitation at 488 nm and green photomultiplier channel; for MitoSOX™ Red: excitation at 420 nm and red photomultiplier channel). Right-hand panel, merged image. Scale bars = 7 μm.

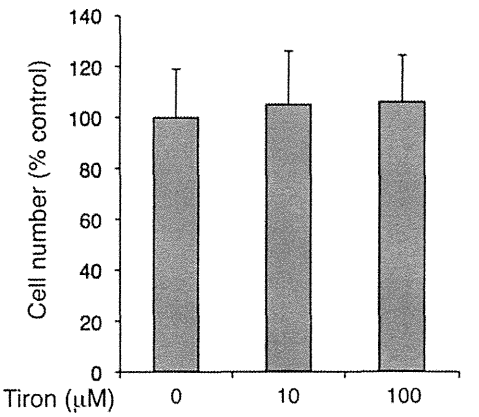

Figure S5 Effect of tiron on C6 cell viability

C6 cells were seeded in a 96-well plate at a density of 10^3 cells/well, followed by stimulated with LPS plus pro-inflammatory cytokines in the presence of the indicated concentrations of tiron for 36 h. The number of viable cells were then determined by cell counting kit. Data are expressed as means ± S.E.M. ($n = 3$).

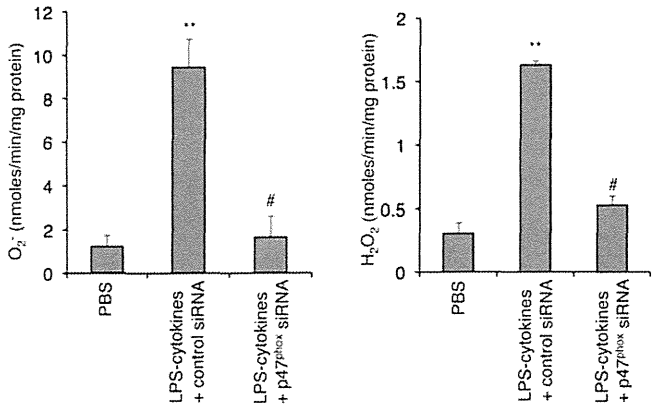

Figure S6 Extracellular concentrations of O_2^- and H_2O_2 and their modulation by $p47^{phox}$ knockdown

C6 cells were seeded in a 12-well plate at a density of 2×10^5 cells/well, followed by treatment with control siRNA or $p47^{phox}$ siRNA or no treatment for 36 h. Cells were then stimulated with LPS plus pro-inflammatory cytokines for a further 36 h. Supernatant obtained from each culture condition was then subjected to O_2^- measurement (cytochrome *c* assay) and H_2O_2 measurement (Xyrenol Orange assay). Data are expressed as means ± S.E.M. ($n = 3$). $^{**}P < 0.01$ compared with control (PBS). $\#P < 0.01$ compared with LPS/cytokines + control siRNA.

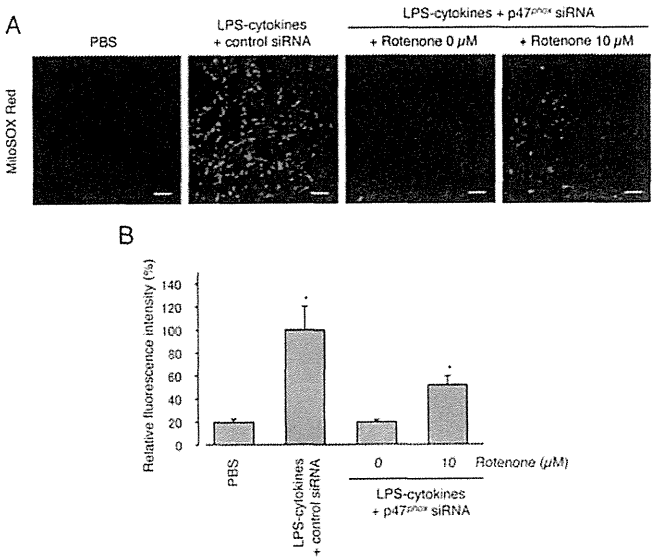

Figure S7 Rotenone induced mitochondrial superoxide in rat C6 glioma cells with Nox2 gene knockdown

Cells were transfected with control siRNA or $p47^{phox}$-specific siRNA as described in the Materials and methods section of the main paper, followed by stimulation with a mixture of LPS (10 μg/ml), IFN-γ (200 units/ml), TNF-α (500 units/ml) and IL-1β (10 ng/ml) for 36 h. Cells transfected with $p47^{phox}$-specific siRNA were treated with 10 μM rotenone or were untreated before stimulation with the LPS-/cytokine mixture. MitoSOX™ Red staining was used to detect mitochondrial superoxide as described in the Materials and methods section of the main paper. (**A**) Fluorescent staining of mitochondrial superoxide. Scale bars = 50 μm. (**B**) Relative fluorescence intensity of C6 cells, treated as described above for MitoSOX™ Red staining. Data are expressed as means ± S.E.M. ($n = 3$). $^{*}P < 0.01$, compared with the PBS-treated group.

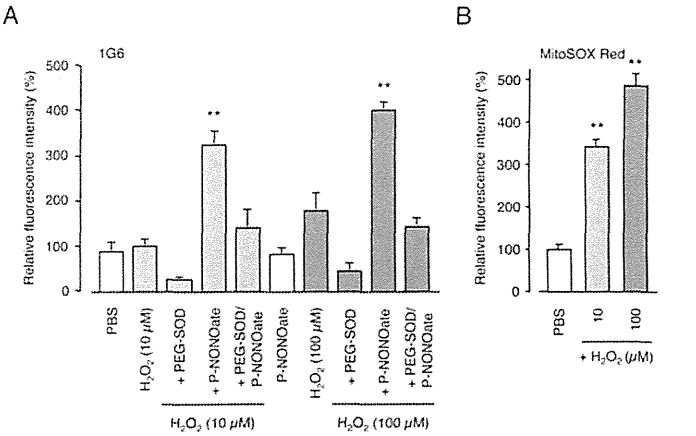

Figure S8 Increase in fluorescence intensity of 8-nitro-cGMP and mitochondrial superoxide in rat C6 glioma cells after H_2O_2 and NO treatment

(**A**) Cells were untreated or treated with 10 or 100 μM H_2O_2 for 36 h, plus PEG–SOD (200 units/ml), P-NONOate (100 μM) or PEG–SOD (200 units/ml) plus P-NONOate (100 μM), and the relative fluorescence intensity of 8-nitro-cGMP was measured using the 1G6 monoclonal antibody, as described in the Materials and methods section. (**B**) In other experiments, cells were untreated or treated with only 10 or 100 μM H_2O_2, followed by determination of the relative fluorescence intensity for MitoSOX™ Red staining compared with the fluorescence intensity of PBS-treated control cells. Data are expressed as means ± S.E.M. ($n = 3$). $^{*}P < 0.01$, compared with the PBS-treated control group.

REFERENCES

1 Pendergrass, W., Wolf, N. and Poot, M. (2004) Efficacy of MitoTracker Green and CMXrosamine to measure changes in mitochondrial membrane potentials in living cells and tissues. Cytometry A **61**, 162–169
2 Akaike, T., Inoue, K., Okamoto, T., Nishino, H., Otagiri, M., Fujii, S. and Maeda, H. (1997) Nanomolar quantification and identification of various nitrosothiols by high performance liquid chromatography coupled with flow reactors of metals and Griess reagent. J. Biochem. **122**, 459–466
3 Li, J.M. and Shah, A.M. (2002) Intracellular localization and preassembly of the NADPH oxidase complex in cultured endothelial cells. J. Biol. Chem. **277**, 19952–19960

Received 24 June 2011/3 October 2011; accepted 4 October 2011
Published as BJ Immediate Publication 4 October 2011, doi:10.1042/BJ20111130

Amino Acids
DOI 10.1007/s00726-010-0535-1

REVIEW ARTICLE

Protein cysteine *S*-guanylation and electrophilic signal transduction by endogenous nitro-nucleotides

Khandaker Ahtesham Ahmed · Tomohiro Sawa · Takaaki Akaike

Received: 16 November 2009 / Accepted: 13 February 2010

Abstract Nitric oxide (NO), a gaseous free radical that is synthesized in organisms by nitric oxide synthases, participates in a critical fashion in the regulation of diverse physiological functions such as vascular and neuronal signal transduction, host defense, and cell death regulation. Two major pathways of NO signaling involve production of the second messenger guanosine 3′,5′-cyclic monophosphate (cGMP) and posttranslational modification (PTM) of redox-sensitive cysteine thiols of proteins. We recently clarified the physiological formation of 8-nitroguanosine 3′,5′-cyclic monophosphate (8-nitro-cGMP) as the first demonstration, since the discovery of cGMP more than 40 years ago, of a new second messenger derived from cGMP in mammals. 8-Nitro-cGMP is electrophilic and reacts efficiently with sulfhydryls of proteins to produce a novel PTM via cGMP adduction, a process that we named protein *S*-guanylation. 8-Nitro-cGMP may regulate electrophilic signaling on the basis of its electrophilicity through induction of *S*-guanylation of redox sensor proteins. Examples include *S*-guanylation of the redox sensor protein Kelch-like ECH-associated protein 1 (Keap1), which leads to activation of NF-E2-related factor 2 (Nrf2)-dependent expression of antioxidant and cytoprotective genes. This *S*-guanylation-mediated activation of an antioxidant adaptive response may play an important role in cytoprotection during bacterial infections and oxidative stress. Identification of new redox-sensitive proteins as targets for *S*-guanylation may help development of novel therapeutics for oxidative stress- and inflammation-related disorders and vascular diseases as well as understanding of cellular protection against oxidative stress.

Keywords Nitric oxide · Reactive oxygen species · Oxidative stress · Posttranslational modification · Redox signal · ROS signal · Electrophilic signal · Adaptive response

K. A. Ahmed · T. Sawa · T. Akaike (✉)
Department of Microbiology, Graduate School of Medical Sciences, Kumamoto University, Kumamoto 860-8556, Japan
e-mail: takakaik@gpo.kumamoto-u.ac.jp

Introduction

Nitric oxide (NO) is one of the smallest and perhaps oldest known bioregulatory molecules. It modulates a number of different cellular functions in prokaryotes, plants, and animals. In stark contrast to the apparent simplicity of this diatomic molecule, its biological chemistry is surprisingly complex, which makes it one of the most versatile signaling molecules known. In the past 20 years, NO has been established as a gaseous free radical with critical and unforeseen roles in quite varied biological functions and organisms (Martinez-Ruiz and Lamas 2009), including regulation of vascular and neuronal signal transduction, host defense, and cell death regulation (Bredt et al. 1990; Mannick 2007; Murad 1986; Patel et al. 2000). In mammals, NO is synthesized by three different NO synthases (NOSs): neuronal NOS (nNOS), inducible NOS (iNOS), and endothelial NOS (eNOS). These NOSs catalyze the oxidation of L-arginine to form NO and L-citrulline (Griffith and Stuehr 1995). Signal transduction of NO can be classified into cGMP-dependent (canonical NO/cGMP pathway) and cGMP-independent [noncanonical: NO-induced posttranslational modifications (PTMs)] (Madhusoodanan and Murad 2007; Martinez-Ruiz and Lamas 2009). The canonical NO/cGMP signaling paradigm involves NO-dependent activation of soluble guanylate cyclase, which results in formation

Published online: 07 March 2010

of cGMP, which itself activates protein kinases, cyclic nucleotide-gated ion channels, and phosphodiesterases (Feelisch 2007; Madhusoodanan and Murad 2007).

NO readily reacts with oxygen radicals and metals to produce chemically reactive compounds named collectively reactive nitrogen oxide species (RNOS). RNOS such as peroxynitrite ($ONOO^-$) and nitrogen dioxide (NO_2) can produce several types of PTMs (Bartesaghi et al. 2007; Eiserich et al. 1998; Radi 2004; Schopfer et al. 2003) including nitration, oxidation, and nitrosylation of amino acid residues in proteins (Akaike 2000; Alvarez and Radi 2003; Yamakura et al. 2005). Protein tyrosine nitration has been associated with several pathological conditions such as neurodegenerative diseases (Beckman et al. 1993), inflammatory airway diseases (Sugiura et al. 2004), and aging (Hong et al., 2007), and hence, regarded as biomarker for biological RNOS formation. Recently, accumulated evidence has suggested that PTMs of redox-sensitive protein thiols contribute to the regulation of NO signaling via cGMP-independent mechanisms (Martinez-Ruiz and Lamas 2009). A well-characterized example of a PTM of redox-sensitive protein thiols by NO is *S*-nitrosylation, i.e., the conjugation of an NO moiety to a reactive cysteine (Cys) thiol (Cys thiolate) to form *S*-nitrosothiol (Akaike 2000; Hess et al. 2005; Stamler et al. 2001).

PTMs mediated by electrophilic metabolites of NO also play an important role in the NO signaling network. Recent studies suggested that biomolecules such as fatty acids and nucleotides react with NO and RNOS to form electrophilic metabolites and that these electrophiles also modify protein thiols to regulate NO signaling. Several groups reported the biological formation of nitrated fatty acids (Baker et al. 2005; Freeman et al. 2008), which has been found to cause thiol modification via *S*-nitroalkylation (Batthyany et al. 2006). However, RNOS are also known to induce nitration of nucleic acids (Fig. 1). During the past several years, nitrated guanine derivatives such as 8-nitroguanine and 8-nitroguanosine were identified in diverse cultured cells and in tissues from humans with lung diseases and different organisms with viral pneumonia, cancer, and other inflammatory conditions (Akaike et al. 2003; Ohshima et al. 2006; Sawa and Ohshima 2006; Sawa et al. 2006; Tazawa et al. 2007; Terasaki et al. 2006; Yasuhara et al. 2005; Yoshitake et al. 2004, 2008). The redox activity of 8-nitroguanosine in particular suggests that guanine nitration may have potent biological effects (Sawa et al. 2003). We recently discovered that another nitrated cyclic nucleotide, 8-nitroguanosine 3′,5′-cyclic monophosphate (8-nitro-cGMP), is produced in cells expressing iNOS (Sawa et al. 2007). 8-Nitro-cGMP has an extremely potent signaling function in biological systems because of its dual nature in signal transduction, i.e., the canonical NO/cGMP pathway and noncanonical electrophilic signaling; among the nitrated guanine derivatives studied, it possessed the strongest redox-active property (Sawa et al. 2007). Because of its potent electrophilic behavior, 8-nitro-cGMP effectively reacts with sulfhydryl groups of particular Cys residues to form a novel PTM via formation of a protein-S-cGMP adduct, named *S*-guanylation (Fig. 2).

In this review article, we will discuss NO-mediated signal transduction and its physiological role in the context of protein Cys thiol modification by the novel nitrated nucleotide derivative 8-nitro-cGMP.

Cys thiol, a prominent target for electrophilic signal transduction

Cys is the most nucleophilic amino acid and readily reacts with oxidants (e.g., reactive oxygen species, ROS) and electrophiles of endogenous and exogenous origins. Not all Cys thiols are important as redox sensors, inasmuch as most protein thiols do not react with oxidants under conditions and at concentrations found in cells. However,

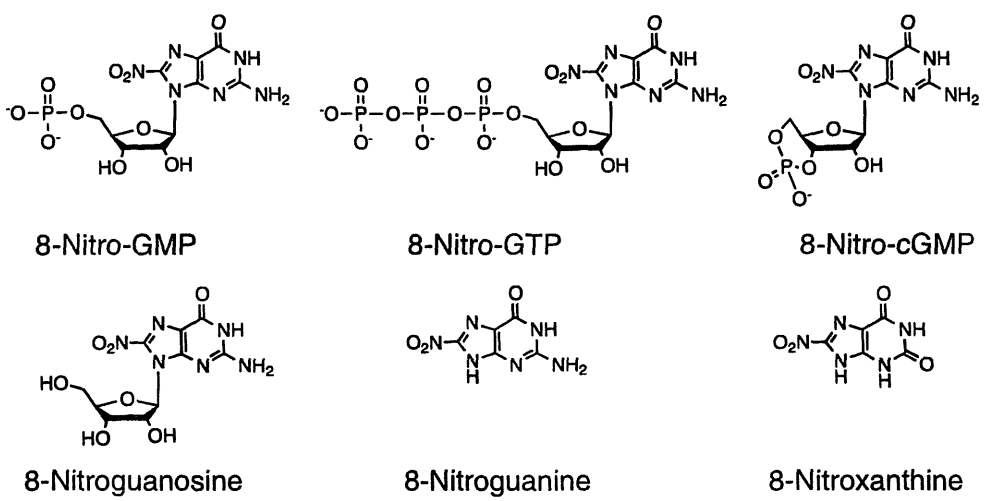

Fig. 1 Chemical structures of 8-nitroguanine-related compounds including various 8-nitroguanine nucleotides

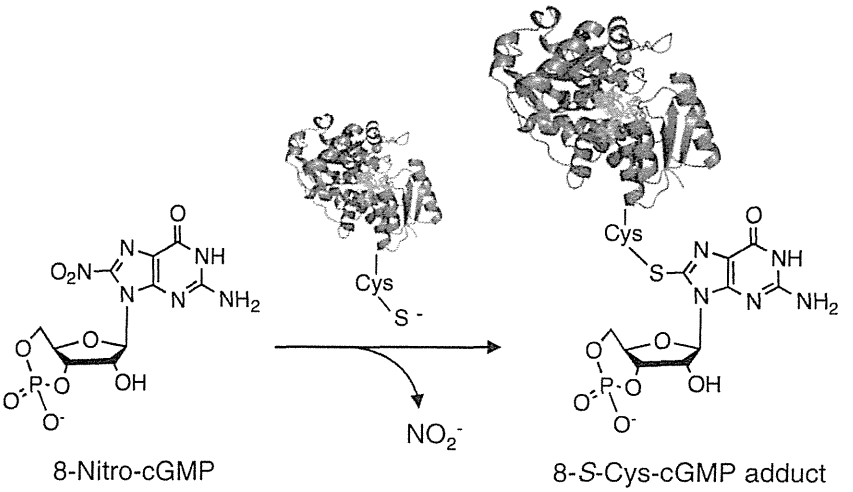

Fig. 2 Schematic representation of protein *S*-guanylation. Nucleophilic protein thiolates attack the C8 carbon of 8-nitro-cGMP, which results in adduction of cGMP moieties to Cys residues in proteins, with concomitant release of nitrite anion

some thiols (i.e., those with low pK_a values) were deprotonated to the thiolate anion state more readily because of their surrounding environment (Eaton 2006). This deprotonation makes these thiols more reactive toward NO, RNOS, and other related electrophiles (Eaton 2006; Winterbourn and Hampton 2008). The pK_a value of the thiol of free Cys is 8.33, and the pK_a values of protein-associated thiols usually stays between 8.2 and 8.5 (Winterbourn and Hampton 2008). The characteristic of the chemical milieu that lowers the pK_a values of Cys thiols is proximity to (a) basic amino acids such as histidine, lysine, and arginine; (b) aromatic amino acids such as tyrosine and tryptophan; or (c) metal centers such as those in heme–metal complexes (Hess et al. 2005; Winterbourn and Hampton 2008). Moreover, protein allostery may affect the accessibility and reactivity of the Cys thiols (Hess et al. 2005; Ishima et al. 2008; Winterbourn and Hampton 2008).

Protein Cys modifications by NO, RNOS, ROS, and related electrophiles include *S*-nitrosylation, *S*-oxidation, and *S*-alkylation. *S*-Nitrosylation is one of the best characterized PTMs associated with NO signaling. A number of proteins have been identified as targets for *S*-nitrosylation, and their functional impact has been extensively studied (Forrester et al. 2009; Hess et al. 2005; Miyamoto et al. 2000). RNOS also react directly with thiol groups. For example, peroxynitrite, a coupling product of NO and superoxide (Szabo et al. 2007), reacts with the thiol group, which results in oxidation of the thiol to form sulfenic acid (RSOH) (Radi et al. 1991). RSOH then reacts with neighboring thiol groups to form intra- or inter-molecular disulfide bonds (Poole et al. 2004). RSOH also plays an important role in glutathionylation, a covalent attachment of glutathione (GSH) to protein thiols via a mixed disulfide bond. *S*-Alkylation results from a reaction with electrophilic secondary metabolites of RNOS. The reaction patterns can be additions or substitutions depending on the structure of the electrophile. Examples of such electrophiles include nitrated fatty acids and nitrated cyclic nucleotides. A number of nitrated fatty acid residues have been found in biological systems and proved as potent as Cys-alkylating electrophilic agents (Baker et al. 2005; Balazy et al. 2001; Batthyany et al. 2006; Freeman et al. 2008; Trostchansky and Rubbo 2006). The nitrated fatty acids have conjugated nitroalkene functions, and the electron-withdrawing nature of the nitro group facilitates the Michael addition of the thiols to the alkenes, which is known as *S*-nitroalkylation (Batthyany et al. 2006).

Cys thiol modification by NO, RNOS, ROS, and RNOS- and ROS-derived electrophiles has been shown to regulate the activity of numerous metabolic enzymes, such as oxidoreductases, proteases, protein kinases, and phosphatases; receptors; ion channels and transporters; and transcription factors. Important regulations of thiol modification-mediated protein functions include (a) inhibition of enzymes by modification of active center thiols; (b) thiol modification-induced functional and structural modulation (allosteric regulation); and (c) regulation of protein–protein interactions (Hess et al. 2005; Jones 2008).

Later in this review, we will provide more details about protein Cys modification by nitro-nucleotides as a novel PTM and its impact on redox signal transduction.

Biological formation of nitrated nucleotides

In vitro and in vivo experiments have identified nitration of nucleic acids (Fig. 1), more specifically guanine derivatives, as associated with various inflammatory conditions. Yermilov et al. (1995) found that peroxynitrite reacts with the guanine base of nucleic acids to form 8-nitroguanine in vitro. Masuda et al. (2002) demonstrated peroxynitrite-mediated 8-nitroguanosine formation from RNA in vitro. Our group first reported in vivo evidence of guanine nitration: we found marked guanine nitration in the lungs of influenza virus-infected mice and human patients with

idiopathic pulmonary fibrosis and lung cancer that depended on production of NO by iNOS (Akaike et al. 2003; Sawa et al. 2006; Terasaki et al. 2006). We also observed formation of 8-nitroguanosine in mice with infections with bacteria such as *Salmonella typhimurium* (Zaki et al. 2009). In addition, Hoki et al. (2007) detected 8-nitroguanine formation in malignant fibrous histiocytoma. Recently, 8-nitroguanine was linked with diabetic retinopathy, which is a major cause of blindness (Yuasa et al. 2008).

Our chemical analyses using high-performance chromatography-based electrochemical detection and tandem mass spectrometry (LC–MS/MS) revealed that a nitrated derivative of cGMP, 8-nitro-cGMP, was generated in significant amounts in cell culture models with different types of cells (Sawa et al. 2007; unpublished observation). For example, 8-nitro-cGMP was identified in the mouse macrophage cell line RAW 264.7 stimulated with cytokines such as interferon-γ and lipopolysaccharide (LPS) to produce NO via iNOS. More important, LC–MS/MS clearly revealed quantitative formation of 8-nitro-cGMP in a rat glioma cell line stimulated with an exogenous NO donor or with LPS plus cytokines (unpublished observation). Infection with the gram-negative bacterium *Salmonella* also facilitated formation of 8-nitro-cGMP in mouse macrophages (Sawa et al. 2007; Zaki et al. 2009). Formation of 8-nitro-cGMP was easily analyzed via immunocytochemistry with the use of anti-8-nitro-cGMP monoclonal antibodies. It was intriguing that immunostaining of intracellular 8-nitro-cGMP colocalized with mitochondria rather than endoplasmic reticulum (Sawa et al. 2007). This intracellular localization may have implications for the mechanism and physiological effects of 8-nitro-cGMP formation. Moreover, this mitochondria-related nitration suggests that 8-nitro-cGMP may have a role as a regulator of mitochondrial functions such as energy metabolism and cell death. 8-Nitro-cGMP formation was also detected with other cultured cells, such as human hepatocellular carcinoma (HepG2) cells, adipocytes, and endothelial cells. Thus, clear evidence now exists that nitrated derivatives of nucleotides are generated under various physiological and pathophysiological conditions, so that they may serve not only as oxidative stress markers but also as biologically functioning electrophilic signal transducers.

Redox signaling property of nitro-nucleotides

8-Nitroguanosine and its derivatives have significant redox activity. In the presence of certain oxidoreductases and electron donors such as NADPH, 8-nitroguanosine derivatives readily reduced to form their anion radicals, which then transferred a single electron to molecular oxygen to form superoxide radical (Akaike et al. 2003; Sawa et al. 2003). 8-Nitro-cGMP had the highest redox activity among the 8-nitroguanosine derivatives tested, with redox activity decreasing in the following order: 8-nitro-cGMP > 8-nitroguanosine > 8-nitroguanosine 5′-monophosphate (8-nitro-GMP) $\approx$ 8-nitroguanosine 5′-triphosphate (8-nitro-GTP). 8-Nitroguanine had only negligible redox activity (Akaike et al. 2003; Sawa et al. 2003, 2007). Oxidoreductases that can reduce 8-nitroguanosines include cytochrome P450 reductase and all three NOS isoforms (Akaike et al. 2003; Sawa et al. 2003).

In view of this redox activity, 8-nitroguanosines may serve to regulate vascular tone. In fact, 8-nitro-cGMP can induce vasoconstriction, possibly through formation of superoxide, as determined in organ bath experiments (Sawa et al. 2007). 8-Nitro-cGMP-induced vasoconstriction depended completely on endothelium, and more specifically on eNOS, which indicates the occurrence of eNOS-dependent reduction of 8-nitro-cGMP to form superoxide, which in turn antagonizes NO-dependent vasorelaxation. At higher concentrations, however, 8-nitro-cGMP induced vasorelaxation, through activation of cGMP-dependent kinase (PKG) in vascular smooth muscle cells.

Nitro-nucleotides: endogenously formed electrophiles

Electrophilicity is another unique property of nitro-nucleotides. Because of their electrophilicity, nitro-nucleotides readily react with nucleophilic thiol compounds of low and high molecular weight to form 8-thioalkoxy-guanosine adducts. We named this unique electrophilic reaction *S*-guanylation of sulfhydryls (Saito et al. 2008; Sawa et al. 2007). This reaction seems to occur via nucleophilic attack by the thiol group of a protein Cys or GSH on the C8 carbon of 8-nitro-cGMP so that the nitro moiety is released and the 8-RS-cGMP adduct is formed (Fig. 2). The major distinction between *S*-guanylation and other *S*-alkylations is that *S*-guanylation is apparently quite stable and produces irreversible sulfhydryl modifications, because the nitro moiety of the purine structure is lost during formation of adducts with protein Cys residues. It is noteworthy that 8-nitro-cGMP is the first known nitrated derivative of a cyclic nucleotide that possesses electrophilicity.

Among the nitroguanine derivatives examined (Fig. 1), 8-nitro-cGMP showed the highest reactivity with thiol compounds. The second-order rate constant for the reaction of 8-nitro-cGMP with the sulfhydryl of GSH was determined to be 0.03 M^{-1} s^{-1} at pH 7.4 and 37°C (Sawa et al. 2007). This value is much smaller than values for other electrophiles such as 4-hydroxynonenal, 15-deoxy-$\Delta^{12,14}$-prostaglandin J_2, and nitro-linoleic and -oleic acids; i.e., those compounds have reaction rate constants with GSH of

1.3, 0.7, 355, 183 M^{-1} s^{-1}, respectively, at pH 7.4 and 37°C. This comparatively lower second-order rate constant may account for the stable nature of this novel compound in the cellular compartment where GSH is abundant (at ~mM levels) and may be responsible for the fact that 8-nitro-cGMP causes very selective *S*-guanylation with sulfhydryls possessing high nucleophilicity, as determined, at least in part, by low pK_a values of sulfhydryls of the Cys moiety.

Protein *S*-guanylation in electrophilic signaling

Because of its electrophilicity, 8-nitro-cGMP may mediate electrophilic signaling via induction of *S*-guanylation of redox sensor proteins. Among this class of proteins, Kelch-like ECH-associated protein 1 (Keap1) was identified as a highly sensitive *S*-guanylation target (Sawa et al. 2007). Keap1 is a negative regulator of NF-E2-related factor 2 (Nrf2), a transcription factor that regulates phase-2 detoxifying and antioxidant enzymes for electrophiles and ROS (Dinkova-Kostova et al. 2005; Motohashi and Yamamoto 2004). The binding of Keap1 to Nrf2 maintains the cytosolic localization of Nrf2 and brings about rapid degradation of Nrf2 by proteasomes. Because Keap1 has highly reactive Cys residues, chemical modification of the sulfhydryl group of Cys residues by electrophiles and ROS has been proposed to decline the ubiquitin ligase activity of Keap1, which would lead to the stabilization and nuclear translocation of Nrf2. Once translocated to nuclei, activated Nrf2 would thus form a heterodimer with small musculoaponeurotic fibrosarcoma (sMaf) and bind to the antioxidant responsive element (ARE) (Fig. 3) to induce expression of various cytoprotective enzymes, which are involved in adaptive responses to oxidative stress (Dinkova-Kostova et al. 2002; Itoh et al. 2004).

Our recent chemical analyses for Keap1 revealed that Keap1 expressed by various cultured cells was highly susceptible to *S*-guanylation induced by NO-dependent 8-nitro-cGMP production (Sawa et al. 2007). In fact, we determined that NO and RNOS can modify Keap1 in macrophages during bacterial infections and in rat glial cells in culture after proinflammatory stimuli. 8-Nitro-cGMP formation was also clearly observed in macrophages infected with the pathogenic bacterium *Salmonella*. *S*-Guanylated Keap1 was then detected in cultured murine macrophages after *Salmonella* infection. These findings are further confirmed by the fact that Keap1 can be exclusively *S*-guanylated by 8-nitro-cGMP produced in vivo in cultured cells (unpublished observation). It is therefore highly plausible that 8-nitro-cGMP may act as an endogenous electrophilic ligand and affect Keap1 sulfhydryls via *S*-guanylation, which would lead to antioxidant signaling (Fig. 3).

We now understand that the Keap1-Nrf2 system can be an important cytoprotective mechanism against electrophiles and ROS (Wakabayashi et al. 2004). Noticeably, cytoprotection and host defense conferred by 8-nitro-cGMP were clearly associated with increased expression of heme oxygenase 1 (HO-1) in macrophages and in vivo during *Salmonella* infection (Zaki et al. 2009). HO-1 is an enzyme with various physiological roles including vasoregulation (Motterlini et al. 1998), cytoprotection (Zuckerbraun et al. 2004), and anti-inflammatory effects (Otterbein et al. 2000). We also reported earlier that HO-1 expression induced by NO contributed to cell survival in certain solid tumor models (Doi et al. 1999; Tanaka et al. 2003). Our present belief that 8-nitro-cGMP may mediate electrophilic signaling via induction of *S*-guanylation was unambiguously supported by our significant data showing that 8-nitro-cGMP directly caused site-specific *S*-guanylation of Keap1, which led to subsequent Nrf2-dependent HO-1 induction with its potent antioxidant effect

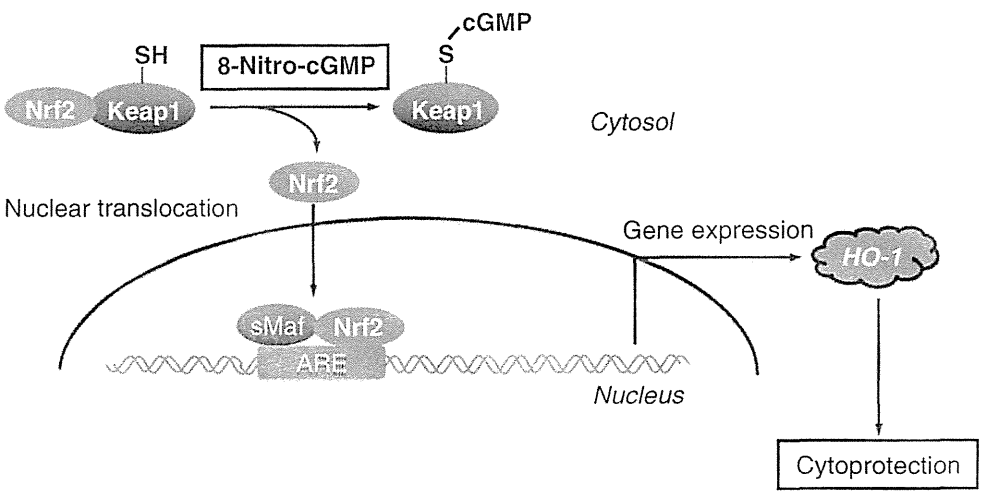

Fig. 3 8-Nitro-cGMP-mediated cytoprotection by *S*-guanylation of Keap1. After *S*-guanylation of Keap1, Nrf2 dissociates from Keap1, is translocated to the nucleus, and acts as a transcription factor in the expression of cytoprotective genes including heme oxygenase-1 (HO-1). *ARE* antioxidant responsive element

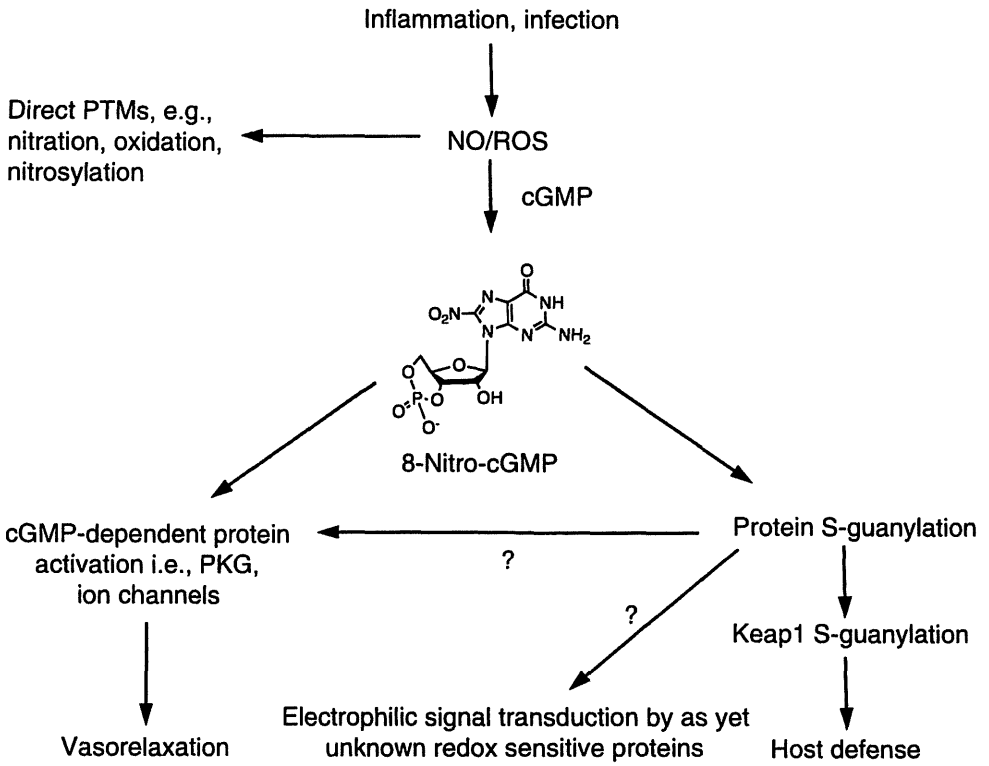

Fig. 4 Signal transduction by 8-nitro-cGMP via protein *S*-guanylation

(unpublished observation). That 8-nitro-cGMP-mediated electrophilic signal transduction may have various effects in the physiology and pathophysiology of NO- and RNOS-related phenomena is therefore conceivable (Sawa et al. 2010) (Fig. 4).

Conclusions

Cys thiol modification constitutes the most important PTM in redox signaling. Inasmuch as Cys thiol modification by an array of RNOS and ROS has been sufficiently explained and researched, that Cys thiol modification plays critical roles in redox signaling is well accepted. *S*-Guanylation is a pretty unique mechanism of protein Cys thiol modification that occurs via electrophilic attack by the recently discovered nitro-nucleotide 8-nitro-cGMP. It is noteworthy that, because RNOS such as $ONOO^-$ has very short half life in physiological condition (less than a second) (Squadrito and Pryor 1998), it can induce direct PTMs including nitration, oxidation, and nitrosylation of various amino acids in the vicinity of its formation. In contrast, 8-nitro-cGMP is relatively stable, and may transduce ROS/RNOS signaling via indirect PTMs (*S*-guanylation) specific to redox-active cysteines. In fact, this electrophilic compound can modify the Cys moiety of redox-sensitive proteins including Keap1, thereby contributing in a critical fashion to redox signaling involving NO-dependent cellular adaptive response mechanisms.

Among approximately 214,000 total Cys residues encoded in the human genome, the redox-sensitive Cys is reported to reach 10–20% (Jones 2008). Thus, a number of proteins containing redox-sensitive thiols remain to be investigated in terms of the 8-nitro-cGMP-mediated PTM *S*-guanylation and their roles in regulating redox signaling. In fact, dozens of proteins that undergo *S*-nitrosylation and *S*-glutathionylation have been described to date (Forrester et al. 2009; Martinez-Ruiz and Lamas 2007). Further analysis is now warranted to achieve comprehensive understanding of target proteins for *S*-guanylation. The recent development of mass spectroscopy-based proteomics may provide a powerful tool for identification of novel redox-sensitive protein targets and the regulation of thiol modification in the cellular milieu.

Acknowledgments We thank Judith B. Gandy for her excellent editing of the manuscript. This work was supported in part by Grants-in-Aid for Scientific Research (B, C: Nos. 21390097, 21590312) and on Innovative Areas (Research in a Proposed Area: Nos. 20117001, 20117005) from the Ministry of Education, Culture, Sports, Science and Technology (MEXT), Japan, by Advanced Education Program for Young Scientists in Integrated Clinical, Basic and Social Medicine, Kumamoto University, and by Grants-in-Aid from the Ministry of Health, Labor and Welfare of Japan.

References

Akaike T (2000) Mechanisms of biological *S*-nitrosation and its measurement. Free Radic Res 33:461–469

Akaike T, Okamoto S, Sawa T, Yoshitake J, Tamura F, Ichimori K, Miyazaki K, Sasamoto K, Maeda H (2003) 8-Nitroguanosine formation in viral pneumonia and its implication for pathogenesis. Proc Natl Acad Sci USA 100:685–690

Alvarez B, Radi R (2003) Peroxynitrite reactivity with amino acids and proteins. Amino Acids 25:295–311

Baker PR, Lin Y, Schopfer FJ, Woodcock SR, Groeger AL, Batthyany C, Sweeney S, Long MH, Iles KE, Baker LM, Branchaud BP, Chen YE, Freeman BA (2005) Fatty acid transduction of nitric oxide signaling: multiple nitrated unsaturated fatty acid derivatives exist in human blood and urine and serve as endogenous peroxisome proliferator-activated receptor ligands. J Biol Chem 280:42464–42475

Balazy M, Iesaki T, Park JL, Jiang H, Kaminski PM, Wolin MS (2001) Vicinal nitrohydroxyeicosatrienoic acids: vasodilator lipids formed by reaction of nitrogen dioxide with arachidonic acid. J Pharmacol Exp Ther 299:611–619

Bartesaghi S, Ferrer-Sueta G, Peluffo G, Valez V, Zhang H, Kalyanaraman B, Radi R (2007) Protein tyrosine nitration in hydrophilic and hydrophobic environments. Amino Acids 32:501–515

Batthyany C, Schopfer FJ, Baker PR, Duran R, Baker LM, Huang Y, Cervenansky C, Branchaud BP, Freeman BA (2006) Reversible post-translational modification of proteins by nitrated fatty acids in vivo. J Biol Chem 281:20450–20463

Beckman JS, Carson M, Smith CD, Koppenol WH (1993) ALS, SOD and peroxynitrite. Nature 364:584

Bredt DS, Hwang PM, Snyder H (1990) Localization of nitric oxide synthase indicating a neural role for nitric oxide. Nature 347:768–770

Dinkova-Kostova AT, Holtzclaw WD, Cole RN, Itoh K, Wakabayashi N, Katoh Y, Yamamoto M, Talalay P (2002) Direct evidence that sulfhydryl groups of Keap1 are the sensors regulating induction of phase 2 enzymes that protect against carcinogens and oxidants. Proc Natl Acad Sci USA 99:11908–11913

Dinkova-Kostova AT, Holtzclaw WD, Kensler TW (2005) The role of Keap1 in cellular protective responses. Chem Res Toxicol 18:1779–1791

Doi K, Akaike T, Fujii S, Tanaka S, Ikebe N, Beppu T, Shibahara S, Ogawa M, Maeda H (1999) Induction of haem oxygenase-1 by nitric oxide and ischaemia in experimental solid tumours and implications for tumour growth. Br J Cancer 80:1945–1954

Eaton P (2006) Protein thiol oxidation in health and disease: techniques for measuring disulfides and related modifications in complex protein mixtures. Free Radic Biol Med 40:1889–1899

Eiserich JP, Hristova M, Cross CE, Jones AD, Freeman BA, Halliwell B, van der Vliet A (1998) Formation of nitric oxide-derived inflammatory oxidants by myeloperoxidase in neutrophils. Nature 391:393–397

Feelisch M (2007) Nitrated cyclic GMP as a new cellular signal. Nat Chem Biol 3:687–688

Forrester MT, Thompson JW, Foster MW, Nogueira L, Moseley MA, Stamler JS (2009) Proteomic analysis of *S*-nitrosylation and denitrosylation by resin-assisted capture. Nat Biotechnol 27:557–559

Freeman BA, Baker PR, Schopfer FJ, Woodcock SR, Napolitano A, d'Ischia M (2008) Nitro-fatty acid formation and signaling. J Biol Chem 283:15515–15519

Griffith OW, Stuehr DJ (1995) Nitric oxide synthases: properties and catalytic mechanism. Annu Rev Physiol 57:707–736

Hess DT, Matsumoto A, Kim SO, Marshall HE, Stamler JS (2005) Protein *S*-nitrosylation: purview and parameters. Nat Rev Mol Cell Biol 6:150–166

Hoki Y, Murata M, Hiraku Y, Ma N, Matsumine A, Uchida A, Kawanishi S (2007) 8-Nitroguanine as a potential biomarker for progression of malignant fibrous histiocytoma, a model of inflammation-related cancer. Oncol Rep 18:1165–1169

Hong SJ, Gokulrangan G, Schoneich C (2007) Proteomic analysis of age dependent nitration of rat cardiac proteins by solution isoelectric focusing coupled to nanoHPLC tandem mass spectrometry. Exp Gerontol 42:639–651

Ishima Y, Akaike T, Kragh-Hansen U, Hiroyama S, Sawa T, Suenaga A, Maruyama T, Kai T, Otagiri M (2008) *S*-Nitrosylated human serum albumin-mediated cytoprotective activity is enhanced by fatty acid binding. J Biol Chem 283:34966–34975

Itoh K, Tong KI, Yamamoto M (2004) Molecular mechanism activating Nrf2-Keap1 pathway in regulation of adaptive response to electrophiles. Free Radic Biol Med 36:1208–1213

Jones DP (2008) Radical-free biology of oxidative stress. Am J Physiol 295:C849–C868

Madhusoodanan KS, Murad F (2007) NO-cGMP signaling and regenerative medicine involving stem cells. Neurochem Res 32:681–694

Mannick JB (2007) Regulation of apoptosis by protein *S*-nitrosylation. Amino Acids 32:523–526

Martinez-Ruiz A, Lamas S (2007) Signalling by NO-induced protein *S*-nitrosylation and *S*-glutathionylation: convergences and divergences. Cardiovasc Res 75:220–228

Martinez-Ruiz A, Lamas S (2009) Two decades of new concepts in nitric oxide signaling: from the discovery of a gas messenger to the mediation of nonenzymatic posttranslational modifications. IUBMB Life 61:91–98

Masuda M, Nishino H, Ohshima H (2002) Formation of 8-nitroguanosine in cellular RNA as a biomarker of exposure to reactive nitrogen oxide species. Chem Biol Interact 139:187–197

Miyamoto Y, Akaike T, Maeda H (2000) *S*-Nitrosylated human α_1-protease inhibitor. Biochim Biophys Acta 1477:90–97

Motohashi H, Yamamoto M (2004) Nrf2-Keap1 defines a physiologically important stress response mechanism. Trends Mol Med 10:549–557

Motterlini R, Gonzales A, Foresti R, Clark JE, Green CJ, Winslow RM (1998) Heme oxygenase-1-derived carbon monoxide contributes to the suppression of acute hypertensive responses in vivo. Circ Res 83:568–577

Murad F (1986) Cyclic guanosine monophosphate as a mediator of vasodilation. J Clin Invest 78:1–5

Ohshima H, Sawa T, Akaike T (2006) 8-Nitroguanine, a product of nitrative DNA damage caused by reactive nitrogen species: formation, occurrence, and implications in inflammation and carcinogenesis. Antioxid Redox Signal 8:1033–1045

Otterbein LE, Bach FH, Alam J, Soares M, Lu HT, Wysk M, Davis RJ, Flavell RA, Choi AMK (2000) Carbon monoxide has anti-inflammatory effects involving the mitogen-activated protein kinase pathway. Nat Med 6:422–428

Patel RP, Moellering D, Murphy-Ullrich J, Jo H, Beckman JS, Darley-Usmar VM (2000) Cell signaling by reactive nitrogen and oxygen species in atherosclerosis. Free Radic Biol Med 28:1780–1794

Poole LB, Karplus PA, Claiborne A (2004) Protein sulfenic acids in redox signaling. Annu Rev Pharmacol Toxicol 44:325–347

Radi R (2004) Nitric oxide, oxidants, and protein tyrosine nitration. Proc Natl Acad Sci USA 101:4003–4008

Radi R, Beckman JS, Bush KM, Freeman BA (1991) Peroxynitrite oxidation of sulfhydryls. The cytotoxic potential of superoxide and nitric oxide. J Biol Chem 266:4244–4250

Saito Y, Taguchi H, Fujii S, Sawa T, Kida E, Kabuto C, Akaike T, Arimoto H (2008) 8-Nitroguanosines as chemical probes of the protein *S*-guanylation. Chem Commun 5984–5986

Sawa T, Ohshima H (2006) Nitrative DNA damage in inflammation and its possible role in carcinogenesis. Nitric Oxide 14:91–100

Sawa T, Akaike T, Ichimori K, Akuta T, Kaneko K, Nakayama H, Stuehr DJ, Maeda H (2003) Superoxide generation mediated by 8-nitroguanosine, a highly redox-active nucleic acid derivative. Biochem Biophys Res Commun 311:300–306

Sawa T, Tatemichi M, Akaike T, Barbin A, Ohshima H (2006) Analysis of urinary 8-nitroguanine, a marker of nitrative nucleic acid damage, by high-performance liquid chromatography-electrochemical detection coupled with immunoaffinity purification: association with cigarette smoking. Free Radic Biol Med 40:711–720

Sawa T, Zaki MH, Okamoto T, Akuta T, Tokutomi Y, Kim-Mitsuyama S, Ihara H, Kobayashi A, Yamamoto M, Fujii S, Arimoto H, Akaike T (2007) Protein *S*-guanylation by the biological signal 8-nitroguanosine 3′,5′-cyclic monophosphate. Nat Chem Biol 3:727–735

Sawa T, Arimoto H, Akaike T (2010) Chemical conjugation of protein thiols by nitric oxide and electrophiles in regulation of redox signaling. Bioconj Chem (in press)

Schopfer FJ, Baker PR, Freeman BA (2003) NO-dependent protein nitration: a cell signaling event or an oxidative inflammatory response? Trends Biochem Sci 28:646–654

Squadrito GL, Pryor WA (1998) Oxidative chemistry of nitric oxide: the roles of superoxide, peroxynitrite, and carbon dioxide. Free Radic Biol Med 25:392–403

Stamler JS, Lamas S, Fang FC (2001) Nitrosylation. The prototypic redox-based signaling mechanism. Cell 106:675–683

Sugiura H, Ichinose M, Tomaki M, Ogawa H, Koarai A, Kitamuro T, Komaki Y, Akita T, Nishino H, Okamoto S, Akaike T, Hattori T (2004) Quantitative assessment of protein-bound tyrosine nitration in airway secretions from patients with inflammatory airway disease. Free Radic Res 38:49–57

Szabo C, Ischiropoulos H, Radi R (2007) Peroxynitrite: biochemistry, pathophysiology and development of therapeutics. Nat Rev Drug Discov 6:662–680

Tanaka S, Akaike T, Fang J, Beppu T, Ogawa M, Tamura F, Miyamoto Y, Maeda H (2003) Antiapoptotic effect of haem oxygenase-1 induced by nitric oxide in experimental solid tumour. Br J Cancer 88:902–909

Tazawa H, Tatemichi M, Sawa T, Gilibert I, Ma N, Hiraku Y, Donehower LA, Ohgaki H, Kawanishi S, Ohshima H (2007) Oxidative and nitrative stress caused by subcutaneous implantation of a foreign body accelerates sarcoma development in *Trp53*$^{+/-}$ mice. Carcinogenesis 28:191–198

Terasaki Y, Akuta T, Terasaki M, Sawa T, Mori T, Okamoto T, Ozaki M, Takeya M, Akaike T (2006) Guanine nitration in idiopathic pulmonary fibrosis and its implication for carcinogenesis. Am J Respir Crit Care Med 174:665–673

Trostchansky A, Rubbo H (2006) Lipid nitration and formation of lipid-protein adducts: biological insights. Amino Acids 32:517–522

Wakabayashi N, Dinkova-Kostova AT, Holtzclaw WD, Kang MI, Kobayashi A, Yamamoto M, Kensler TW, Talalay P (2004) Protection against electrophile and oxidant stress by induction of the phase 2 response: fate of cysteines of the Keap1 sensor modified by inducers. Proc Natl Acad Sci USA 101:2040–2045

Winterbourn CC, Hampton MB (2008) Thiol chemistry and specificity in redox signaling. Free Radic Biol Med 45:549–561

Yamakura F, Matsumoto T, Ikeda K, Taka H, Fujimura T, Murayama K, Watanabe E, Tamaki M, Imai T, Takamori K (2005) Nitrated and oxidized products of a single tryptophan residue in human Cu, Zn-superoxide dismutase treated with either peroxynitrite-carbon dioxide or myeloperoxidase-hydrogen peroxide-nitrite. J Biochem 138:57–69

Yasuhara R, Miyamoto Y, Akaike T, Akuta T, Nakamura M, Takami M, Morimura N, Yasu K, Kamijo R (2005) Interleukin-1β induces death in chondrocyte-like ATDC5 cells through mitochondrial dysfunction and energy depletion in a reactive nitrogen and oxygen species-dependent manner. Biochem J 389:315–323

Yermilov V, Rubio J, Ohshima H (1995) Formation of 8-nitroguanine in DNA treated with peoxynitrite in vitro and its rapid removal from DNA by depurination. FEBS Lett 376:207–210

Yoshitake J, Akaike T, Akuta T, Tamura F, Ogura T, Esumi H, Maeda H (2004) Nitric oxide as an endogenous mutagen for Sendai virus without antiviral activity. J Virol 78:8709–8719

Yoshitake J, Kato K, Yoshioka D, Sueishi Y, Sawa T, Akaike T, Yoshimura T (2008) Suppression of NO production and 8-nitroguanosine formation by phenol-containing endocrine-disrupting chemicals in LPS-stimulated macrophages: involvement of estrogen receptor-dependent or -independent pathways. Nitric Oxide 18:223–228

Yuasa I, Ma N, Matsubara H, Fukui Y, Uji Y (2008) Inducible nitric oxide synthase mediates retinal DNA damage in Goto-Kakizaki rat retina. Jpn J Ophthalmol 52:314–322

Zaki MH, Fuji S, Okamoto T, Islam S, Khan S, Ahmed KA, Sawa T, Akaike T (2009) Cytoprotective function of heme oxygenase 1 induced by a nitrated cyclic nucleotide formed during murine salmonellosis. J Immunol 182:3746–3756

Zuckerbraun BS, Billiar TR, Otterbein SL, Kim PK, Liu F, Choi AM, Bach FH, Otterbein LE (2004) Carbon monoxide protects against liver failure through nitric oxide-induced heme oxygenase 1. J Exp Med 198:1707–1716

Human Molecular Genetics, 2012, Vol. 21, No. 15 **3489–3499**
doi:10.1093/hmg/dds180
Advance Access published on May 15, 2012

Alterations of social interaction through genetic and environmental manipulation of the 22q11.2 gene *Sept5* in the mouse brain

Kathryn M. Harper[1], Takeshi Hiramoto[2], Kenji Tanigaki[4], Gina Kang[2], Go Suzuki[2], William Trimble[5] and Noboru Hiroi[1,2,3,*]

[1]Dominick P. Purpura Department of Neuroscience, [2]Department of Psychiatry and Behavioral Sciences and [3]Department of Genetics, Albert Einstein College of Medicine, 1300 Morris Park Avenue, Bronx, NY 10461, USA, [4]Research Institute, Shiga Medical Center, 5-4-30 Moriyama, Moriyama-shi, Shiga, Japan and [5]Program in Cell Biology, Hospital for Sick Children, 555 University Avenue, Toronto, Ontario, Canada M5G 1X8

Received March 30, 2012; Revised and Accepted May 10, 2012

Social behavior dysfunction is a symptomatic element of schizophrenia and autism spectrum disorder (ASD). Although altered activities in numerous brain regions are associated with defective social cognition and perception, the causative relationship between these altered activities and social cognition and perception—and their genetic underpinnings—are not known in humans. To address these issues, we took advantage of the link between hemizygous deletion of human chromosome 22q11.2 and high rates of social behavior dysfunction, schizophrenia and ASD. We genetically manipulated *Sept5*, a 22q11.2 gene, and evaluated its role in social interaction in mice. *Sept5* deficiency, against a high degree of homogeneity in a congenic genetic background, selectively impaired active affiliative social interaction in mice. Conversely, virally guided overexpression of *Sept5* in the hippocampus or, to a lesser extent, the amygdala elevated levels of active affiliative social interaction in C57BL/6J mice. Congenic knockout mice and mice overexpressing Sept5 in the hippocampus or amygdala were indistinguishable from control mice in novelty and olfactory responses, anxiety or motor activity. Moreover, post-weaning individual housing, an environmental condition designed to reduce stress in male mice, selectively raised levels of Sept5 protein in the amygdala and increased active affiliative social interaction in C57BL/6J mice. These findings identify this 22q11.2 gene in the hippocampus and amygdala as a determinant of social interaction and suggest that defective social interaction seen in 22q11.2-associated schizophrenia and ASD can be genetically and environmentally modified by altering this 22q11.2 gene.

INTRODUCTION

The ability to socially interact with others has a fundamental biological significance in humans and other species. Its biological role is appreciated in social behavior dysfunctions seen in developmental neuropsychiatric disorders. Social dysfunction is a prodromal and symptomatic element of schizophrenia (1) and autism spectrum disorder (ASD) throughout its developmental course toward adulthood (2).

Individuals with 3 Mb and nested 1.5 Mb hemizygosity of 22q11.2 exhibit extraordinarily high rates of social behavior deficits (3–9), schizophrenia (10–17) and ASD (8,18–22). Moreover, social behavior dysfunction precedes (5)–and its severity is associated with (17,23)–the emergence of schizophrenia among individuals with 22q11.2 hemizygosity. This chromosomal locus is one of many sites of copy number variations associated with ASD (24–33) and schizophrenia (16,33–42).

*To whom correspondence should be addressed at: Department of Psychiatry and Behavioral Sciences, Dominick P. Purpura Department of Neuroscience, Department of Genetics, Albert Einstein College of Medicine, Golding 104, 1300 Morris Park Avenue, Bronx, NY 10461, USA. Tel: +1 7184303124; Fax: +1 7184303125; Email: noboru.hiroi@einstein.yu.edu

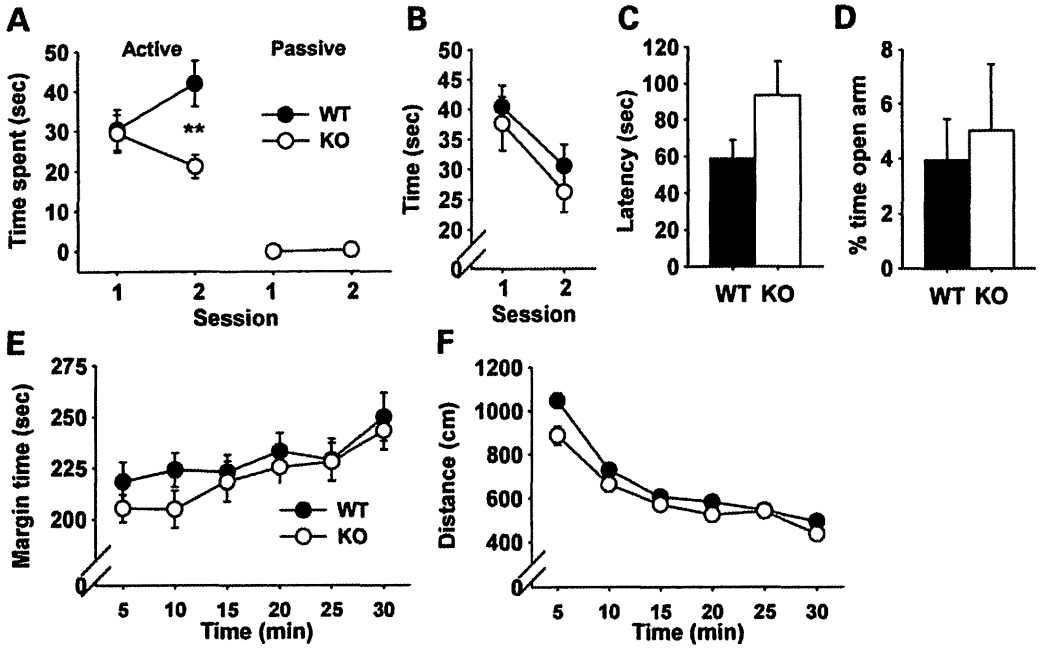

Figure 1. Effects of genetic *Sept5* deficiency on behavior. Data are presented as means ± SEM. (**A**) Active and passive social interactions. Whether the two groups (KO and WT pairs) differed depended on the type of social behavior (active versus passive) and session (group × session, $F_{1,26} = 7.53$, $P = 0.0109$; group × social type × session, $F_{1,26} = 7.50$, $P = 0.011$). Although the active social interaction category included both active affiliative and aggressive social behaviors, mice overwhelmingly exhibited active affiliative social interaction (100% in WT and 100% in KO). Asterisks indicate a statistically significant difference of 1%, as determined by the Newman–Keuls comparison. WT, $n = 14$; KO, $n = 14$. (**B**) Time spent contacting a novel object. The two genotype groups were indistinguishable and their contact time equally declined from the first to the second session (genotype, $F_{1,16} = 0.14$, $P = 0.716$; session, $F_{1,16} = 16.67$, $P = 0.0009$; genotype × session, $F_{1,16} = 0.28$, $P = 0.6036$). WT, $n = 7$; KO, $n = 11$. (**C**) Latency to find buried food. The two genotype groups did not differ ($t(26) = 1.58$, $P = 0.1267$). WT, $n = 13$; KO, $n = 15$. The slightly higher value in the KO group was partly due to one outlier that did not find the food during the test session (see Supplementary Material, Fig. S1). (**D**) The relative amounts of time spent in the open arms over both open and closed arms in the elevated plus maze (EPM). The two genotype groups were indistinguishable in the relative time spent in ($t(23) = 0.39$, $P = 0.7011$) and frequency of visits to ($t(23) = 0.16$, $P = 0.8769$, not shown for clarity) the open arms. WT, $n = 14$; KO, $n = 11$. (**E**) Thigmotaxis. The two genotype groups were indistinguishable in time spent in the margin area of the inescapable open field, and this equally increased during the session (genotype, $F_{1,33} = 0.78$, $P = 0.3832$; time, $F_{5,165} = 6.33$, $P < 0.0001$; $F_{5,165} = 0.42$, $P = 0.8348$). WT, $n = 19$; KO, $n = 16$. (**F**) Motor activity in an open field. The two groups were indistinguishable and equally reduced motor activity during the session (genotype, $F_{1,33} = 2.72$, $P = 0.1089$; time, $F_{5,165} = 86.57$, $P < 0.0001$; genotype × time, $F_{10,165} = 1.85$, $P = 0.105$). WT, $n = 19$; KO, $n = 16$.

Because 22q11.2 hemizygous deletions minimally include approximately 30 genes, the precise manner by which individual 22q11.2 genes functionally contribute to the etiology of social interaction deficits, schizophrenia and ASD cannot be ascertained in humans. As this human chromosomal region is conserved in the mouse, a genetic mouse model is one reliable way to circumvent this problem. Previous studies have identified a 200 kb region of 22q11.2 whose gene dose alteration induces social behavior dysfunction and antipsychotic-responsive behavioral abnormalities (43) and prepulse inhibition deficits (44) in mice. Subsequently, we identified *Sept5*, one of the four encoded genes in the 200 kb region, as a determinant for social interaction in mice (45). Recently, one child has been identified with homozygous deletion of *SEPT5* and its adjacent *GP1BB*, and this patient exhibits deficits in socio-emotional function and language and speech development (46). Although this single case study is consistent with the hypothesis that *SEPT5* deficiency causes ASD- and schizophrenia-related phenotypes, more cases are needed to establish the degree of association between this mutation and neuropsychiatric disorders. Moreover, because the two genes are deleted in this individual, whether *SEPT5* alone contributes to these various symptoms remains unclear.

In the present study, we took advantage of our identification of the murine *Sept5* gene as a risk factor for defective social interaction to further advance our understanding of the role of this 22q11.2 gene in social behavior. Our analysis shows that Sept5 levels in the hippocampus and amygdala act as a determinant of social interaction in mice.

RESULTS

Sept5 deficiency decreases affiliative social interaction

Although our previous study showed that genetic background affects the penetrance of *Sept5* deficiency (45), an alternative interpretation is that the phenotypic difference between wild-type (WT) and knockout (KO) mice reflects unequal distributions of background alleles between the genotypes, rather than the genuine impact of *Sept5* deficiency. To evaluate the impact of constitutive *Sept5* deficiency on social interaction against a much higher level of homogeneous genetic background than our *Sept5* KO mice (45), we developed a congenic *Sept5*-deficient mouse on a C57BL/6J background and tested its behavior. Congenic KO mice showed lower levels of active affiliative social interaction during the second session than WT littermates (Fig. 1A). The phenotype in social interaction

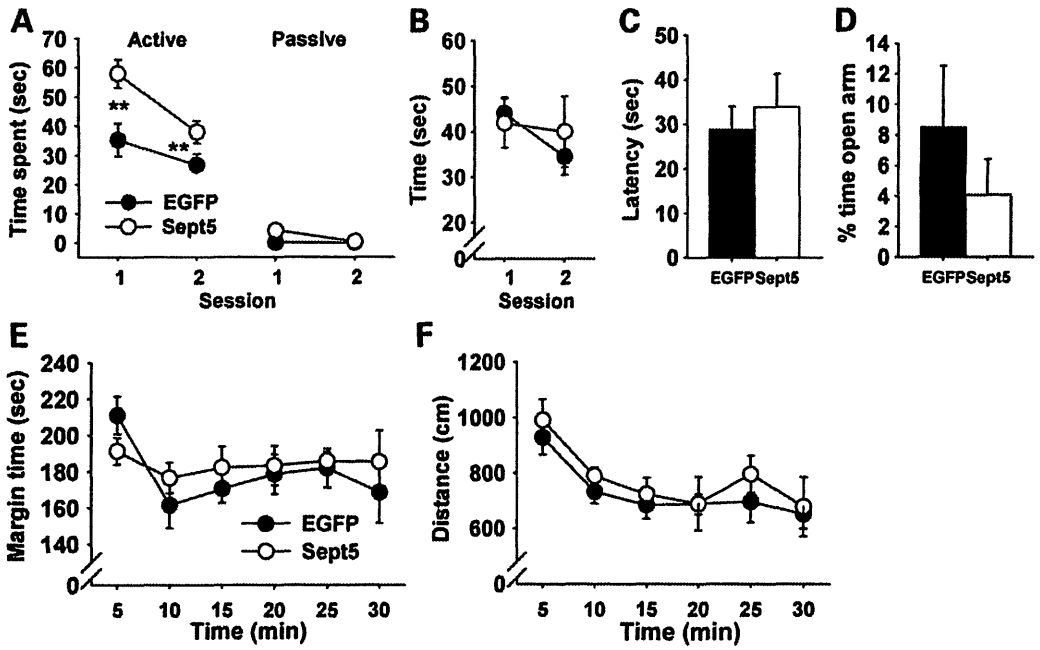

Figure 2. Behavioral effects of virally overexpressed *Sept5* in the dorsal hippocampus. (A) Active and passive social interactions. *Sept5*-infused mice spent more time in active social interaction; there was no difference between the two vector groups in passive social interaction (group, $F_{1,15} = 9.63$, $P = 0.0073$; social type, $F_{1,15} = 162.73$, $P < 0.0001$; session, $F_{1,15} = 47.13$, $P < 0.0001$; group × social type, $F_{1,15} = 6.12$, $P = 0.0258$; group × session, $F_{1,15} = 10.02$, $P = 0.0064$; group × type × session, $F_{1,15} = 3.13$, $P = 0.097$). **Significant at the 1% level, as determined by Newman–Keuls comparisons. Ninety-nine percent and 98% of active social interaction was non-aggressive, active affiliative social interaction in EGFP- and Sept5-infused mice, respectively. EGFP, $n = 9$; Sept5, $n = 8$. (**B**) Time spent contacting a novel object. *Sept5* infusion had no effect on this behavior (group, $F_{1,15} = 0.055$, $P = 0.8177$; session, $F_{1,15} = 5.49$, $P = 0.0333$; group × session, $F_{1,15} = 2.45$, $P = 0.1381$). EGFP, $n = 9$; Sept5, $n = 8$. (**C**) Latency to find buried food. The two groups did not differ ($t(15) = 0.58$, $P = 0.5707$). EGFP, $n = 9$; Sept5, $n = 8$. (**D**) EPM. The two groups did not differ in percent of time spent in ($t(11) = 0.90$, $P = 0.3864$) and percent visits to ($t(11) = 1.30$, $P = 0.2186$, not shown for clarity) the open arms. EGFP, $n = 7$; Sept5, $n = 6$. (**E**) Thigmotaxis. The two groups were indistinguishable and were stable during the entire session (group, $F_{1,15} = 0.38$, $P = 0.5461$; time, $F_{5,75} = 2.13$, $P = 0.0709$; group × time, $F_{5,75} = 0.80$, $P = 0.5518$). EGFP, $n = 9$; Sept5, $n = 8$. (**F**) Motor activity in an open field. The two groups were indistinguishable and stably decreased their locomotor activity during the session (group, $F_{1,15} = 0.76$, $P = 0.3969$; time, $F_{5,75} = 6.76$, $P < 0.0001$; group × time, $F_{5,75} = 0.167$, $P = 0.974$). EGFP, $n = 9$; Sept5, $n = 8$.

did not primarily reflect alterations in non-specific elements of social behavior, as no phenotype was found in their approach behavior to a novel object (Fig. 1B), olfactory functioning in the buried food test (Fig. 1C), anxiety-like behavior in an elevated plus maze (Fig. 1D) and thigmotaxis (Fig. 1E) and general motor activity in the open field (Fig. 1F).

Virally guided overexpression of Sept5 in neurons in the hippocampus and amygdala of C57BL/6J mice increases affiliative social interaction

A corollary of our observation with congenic *Sept5* KO mice is that heightened expression of Sept5 protein in the mouse brain causes high levels of social interaction. Although Sept5 protein is expressed throughout the mouse and human brain (47,48), we targeted limbic regions for their implicated roles in social behavior. To selectively manipulate *Sept5* in distinct brain regions, we constructed a lentiviral vector carrying *Sept5* and surgically infused it into the brains of C57BL/6J mice. Compared with enhanced green fluorescent protein (EGFP), Sept5 overexpression in the hippocampus (Fig. 2A) and amygdala (Fig. 3A) increased active affiliative social interaction in C57BL/6J mice. This phenotype was highly selective, as Sept5 overexpression had no effect on novel object exploration (Figs 2B and 3B), latency to find buried food (Figs 2C and 3C), anxiety-related behaviors in the elevated plus maze (Figs 2D and 3D) and thigmotaxis (Figs 2E and 3E) or motor behavior in the open field (Figs 2F and 3F).

Although there were occasional dorsal spreads of EGFP, along needle tracks, within the somatosensory cortex of the hippocampus- and amygdala-infusion groups (Supplementary Material, Fig. S2A and B), selective infusion of the vector into the somatosensory cortex (Supplementary Material, Fig. S2C) had no effect on any of these behaviors (Fig. 4A and C–F), except that *Sept5* infusion into this cortical area facilitated novel object approach (Fig. 4B).

Gene expression, as identified by EGFP, was centered in the CA2/CA3 of the dorsal hippocampus (Fig. 5A; Supplementary Material, Fig. S2A), the basolateral amygdaloid complex (Fig. 5C; Supplementary Material, Fig. S2B) or the somatosensory cortex (Supplementary Material, Fig. S2C). Consistent with the relatively higher levels of CamkIIα promoter activity in the hippocampus than in the amygdala (49), more widespread gene expression was seen in the former than the latter region (Fig. 5A and C). Gene expression was observed in neurons, as labeled by NeuN (Fig. 5B and D).

Post-weaning individual housing raises Sept5 levels in the amygdala and increases active affiliative social interaction in C57BL/6J mice

Individuals with identical 22q11.2 hemizygosity vary in the presence, onset and severity of social dysfunctions and

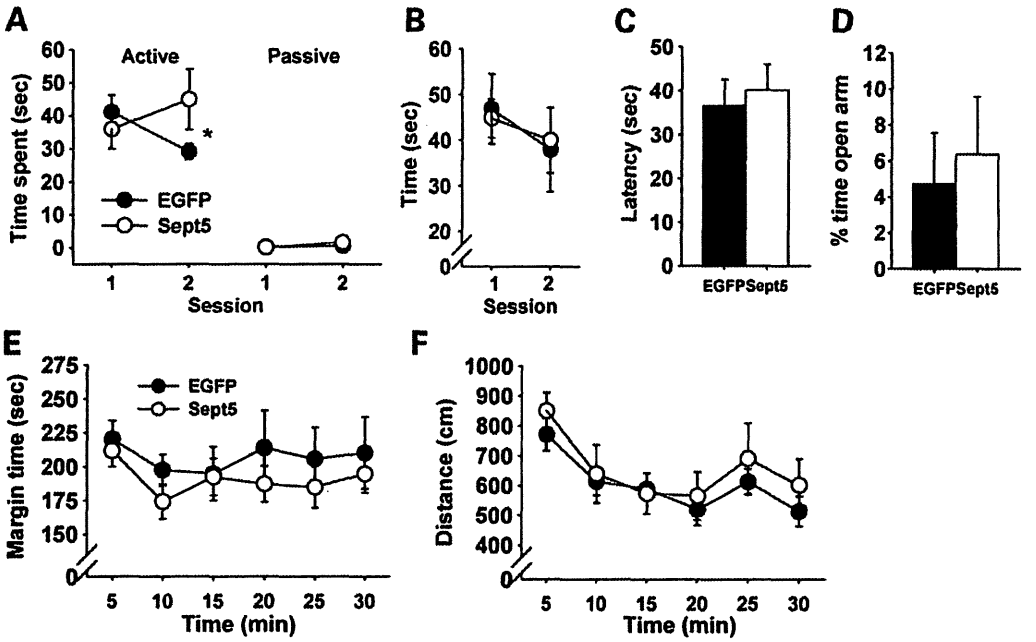

Figure 3. Behavioral effects of virally overexpressed *Sept5* in the basolateral amygdaloid complex. (**A**) Active and passive social interactions. Whether EGFP- and Sept5-infused groups differed depended on the type of social behavior (active versus passive) and session (group, $F_{1,16} = 0.67$, $P = 0.4236$; group × type, $F_{1,16} = 0.45$, $P = 0.5101$; group × session, $F_{1,16} = 12.32$, $P = 0.0029$; group × social type × session, $F_{1,16} = 9.20$, $P = 0.0079$). *Post hoc* comparisons showed that, compared with EGFP mice, Sept5-infused mice showed higher levels of active social interaction at the second session (*significant at the 5% level). An analysis of raw data showed that EGFP and Sept5 mice exhibited active affiliative social interaction in 99 and 84%, respectively, in all active social interaction. EGFP, $n = 10$; Sept5, $n = 8$. (**B**) Time spent contacting a novel object. The treatment had no effect on novel object exploration (group, $F_{1,13} = 0.00001$, $P = 0.998$; session, $F_{1,13} = 4.18$, $P = 0.0616$; group × session, $F_{1,13} = 0.38$, $P = 0.5485$). EGFP, $n = 9$; Sept5, $n = 6$. (**C**) Latency to find buried food. The two groups were indistinguishable in this behavior ($t(12) = 0.41$, $P = 0.6884$). EGFP, $n = 8$; Sept5, $n = 6$. (**D**) The relative amounts of time spent in the open arms over both open and closed arms of the EPM. The two groups did not differ in percent of time spent in ($t(11) = 0.38$, $P = 0.7079$) and percent visits to ($t(11) = 0.59$, $P = 0.5665$, not shown for clarity) the open arms. EGFP, $n = 7$; Sept5, $n = 6$. (**E**) Thigmotaxis. The groups were indistinguishable and were stable during the entire session (group, $F_{1,12} = 1.02$, $P = 0.3334$; time, $F_{5,60} = 0.93$, $P = 0.4708$; group × time, $F_{5,60} = 0.19$, $P = 0.9641$). EGFP, $n = 7$; Sept5, $n = 7$. (**F**) Motor activity in an open field. The treatment groups were indistinguishable and stably decreased their locomotor activity during the session (group, $F_{1,12} = 0.38$, $P = 0.5512$; time, $F_{5,60} = 10.08$, $P < 0.0001$; group × time, $F_{5,60} = 0.42$, $P = 0.8353$). EGFP, $n = 7$; Sept5, $n = 7$.

developmental neuropsychiatric disorders (5–9). Environmental factors, such as stress, have been suggested to contribute to the onset of neuropsychiatric disorders and behavioral/neurocognitive deficits (50), but it is difficult to isolate the precise environmental factor in humans. Unlike rats, male mice are highly territorial and intolerant against same-sex conspecifics, and frequently exhibit inter-individual aggression when group-housed (51). We took advantage of the well-documented effect of post-weaning individual housing to reduce anxiety and increase affiliative social interaction in male mice (52–55).

Post-weaning individual housing selectively raised Sept5 protein levels in the amygdala (Fig. 6A and B). No alteration was seen in the prefrontal cortex, nucleus accumbens, caudate-putamen, hippocampus, ventral tegmental area (VTA) and substantia nigra.

Post-weaning individual housing increased active affiliative social interaction (Fig. 7A), but had no effect on a novel object approach (Fig. 7B) or the buried food search (Fig. 7C). In contrast, individual housing decreased anxiety-related behaviors in the elevated plus maze (Fig. 7D) and thigmotaxis in an inescapable open field (Fig. 7E), and elevated basal levels of motor activity in the open field, but not the rate of habituation of motor activity (Fig. 7F).

DISCUSSION

Our results provide three lines of evidence to support the hypothesis that *Sept5*, a 22q11.2 gene, is a determinant for affiliative social interaction in mice. First, constitutive homozygosity of *Sept5* reduced levels of active affiliative social interaction in congenic KO mice compared with WT mice. Second, virally guided overexpression of *Sept5* in the hippocampus or amygdala enhanced social interaction in C57BL/6J mice. The impact of Sept5 alterations on active affiliative social interaction was highly selective and was not attributable to alterations in novel object exploration, olfactory investigation, anxiety-related behaviors or motor activity. Third, post-weaning individual housing, a condition known to reduce stress in male mice, selectively elevated Sept5 protein levels in the amygdala and increased active affiliative social interaction.

Defective social interaction is the primary symptom of ASD and a prodromal and symptomatic element of schizophrenia (1,5,17,23). Although a repetitive behavioral tendency is another symptomatic element of these neuropsychiatric disorders, neither non-congenic *Sept5*-deficient mice (45) nor congenic *Sept5* KO mice (data not shown) exhibited such a

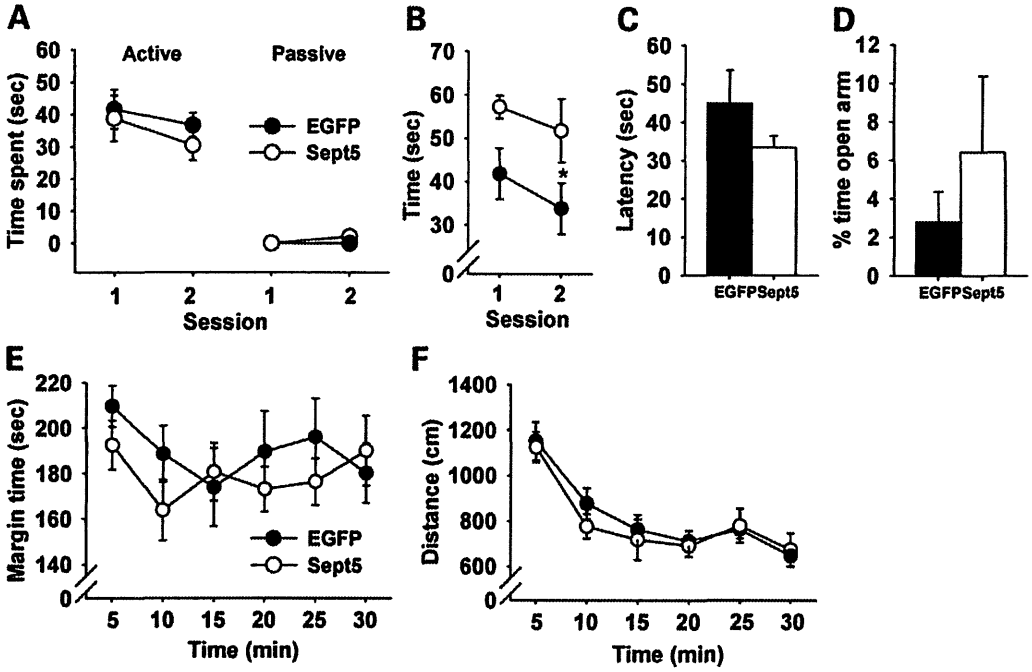

Figure 4. Behavioral effects of virally overexpressed *Sept5* in the somatosensory cortex. (**A**) Active and passive social interactions. Sept5 infused into the somatosensory cortex had no effect on social interaction (group, $F_{1,17} = 0.37$, $P = 0.5535$; social type, $F_{1,17} = 115.75$, $P < 0.0001$; session, $F_{1,17} = 1.42$, $P = 0.2495$; group × social type, $F_{1,17} = 0.65$, $P = 0.4306$; group × session, $F_{1,17} = 0.03$, $P = 0.8603$; group × type × session, $F_{1,17} = 0.46$, $P = 0.5077$). Ninety-eight percent and 100% of active social interaction was non-aggressive, affiliative social interaction in EGFP- and Sept5-infused mice, respectively. EGFP, $n = 10$; Sept5, $n = 9$. (**B**) Time spent contacting a novel object. Sept5 infusion into the somatosensory cortex raised levels of approach toward a novel object (group, $F_{1,17} = 5.87$, $P = 0.0269$; session, $F_{1,17} = 2.48$, $P = 0.1338$; group × session, $F_{1,17} = 0.09$, $P = 0.7683$). EGFP, $n = 10$; Sept5, $n = 9$. (**C**) Latency to find buried food. Sept5 expression in the somatosensory cortex had no effect on this test of olfactory functioning ($t(17) = 1.19$, $P = 0.2496$). EGFP, $n = 10$; Sept5, $n = 9$. (**D**) EPM. The two groups did not differ in percent of time spent in ($t(12) = 0.85$, $P = 0.4112$) and percent visits to ($t(12) = 0.55$, $P = 0.5921$) the open arms. EGFP, $n = 7$; Sept5, $n = 7$. (**E**) Thigmotaxis. Sept5 overexpression in the somatosensory cortex had no effect on thigmotaxis (group, $F_{1,14} = 0.56$, $P = 0.4673$; time, $F_{5,70} = 1.53$, $P = 0.1919$; group × time, $F_{5,70} = 1.01$, $P = 0.4205$). EGFP, $n = 8$; Sept5, $n = 8$. (**F**) Motor activity in an open field. Sep5 overexpression in the somatosensory cortex had no effect on locomotor activity (group, $F_{1,14} = 0.12$, $P = 0.7366$; time, $F_{5,70} = 31.11$, $P < 0.0001$; group × time, $F_{5,70} = 0.548$, $P = 0.7392$). EGFP, $n = 8$; Sept5, $n = 8$.

behavioral trait in spontaneous alternation or rewarded alternation. Given that heterozygosity of *Tbx1*, another 22q11.2 gene, causes both social interaction deficits and a repetitive behavioral trait (56), we suggest that more than one 22q11.2 gene impact multiple or single symptomatic elements of 22q11.2-associated schizophrenia and ASD.

Sept5 was the first 22q11.2 gene whose deficiency was found to reduce levels of affiliative social interaction in mice (45). Our previous study showed that social interaction deficits were present in mice with a mixed genetic background of CD1, 129X1/SvJ and 129S1, but were absent when the genetic background was shifted toward 129X1/SvJ (45). Our present data show that after achieving a highly homogeneous genetic background with C57BL/6J mice, congenic *Sept5* KO mice still exhibit affiliative social interaction deficits. Moreover, overexpression of *Sept5*, against the co-isogenic genetic background, in the brains of C57BL/6J mice elevated levels of affiliative social interaction. These observations lend further support to the hypothesis that *Sept5* is indeed a determinant of social interaction and that genetic background influences its phenotypic penetrance. This provides a plausible explanation for the clinical observation that not all individuals with identical 22q11.2 hemizygous deletions exhibit social behavior deficits, and those with this phenotype exhibit varying degrees of phenotypic severity (5–9).

A decrease in time spent in social interaction is usually seen from the first to second sessions and is thought to reflect recognition memory. C57BL/6J mice infused with EGFP alone showed this habituation, but congenic *Sept5* WT mice instead showed higher levels of active social interaction in the second session than in the first session, despite the fact that congenic WT mice carry a C57BL/6J genetic background. As even after 10 generations of back-crossing congenic WT mice and the donor inbred strain are not genetically identical (57), allelic differences between congenic WT mice and C57BL/6J mice might have contributed to the baseline difference.

Virally guided overexpression of *Sept5* in the hippocampus increased the overall level of active affiliative social interaction, and EGFP- and Sept5-infused mice showed similar rates of habituation. In contrast, virally guided overexpression of *Sept5* in the amygdala elevated levels of active affiliative social interaction in the second, but not first session. The reason for this selective elevation of social interaction in the second session in the amygdala group is not clear. One possibility is that, as the stimulus mice exhibit less active social interaction, mice in the Sept5 amygdala group reactively exhibit more active social interaction. However, our data do not support this interpretation; although such a trend would show as a negative correlation in time spent in social interaction between Sept5 amygdala mice and stimulus mice,

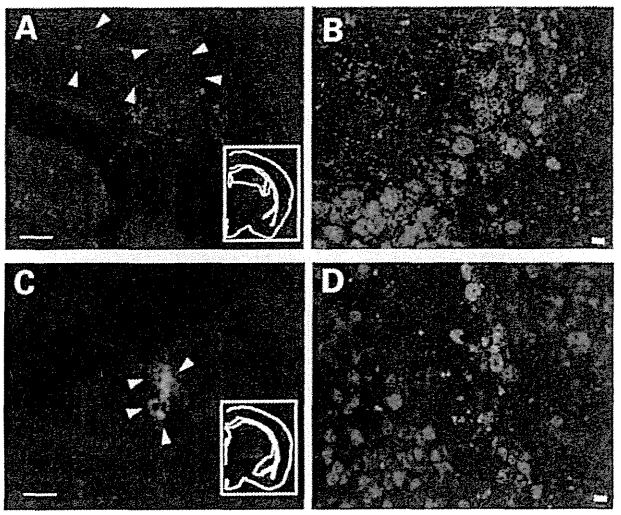

Figure 5. (**A** and **C**) EGFP expression, indicated by arrows, in mice infused with $P_{CamkIIα}$-*Sept5-IRES-EGFP* into the hippocampus (A) and amygdala (C). Because Sept5 staining does not distinguish endogenous Sept5 and exogenously expressed Sept5, EGFP was used to identify areas where Sept5 was overexpressed. Insets indicate the area from which the image was taken; the viral particles were expressed in the dorsal hippocampus and the basolateral amygdaloid complex. Scale bar: 500 μm. (**B** and **D**) Confocal image of EGFP (green) and NeuN (red) in the CA2/3 region of the hippocampus (B) and basolateral amygdaloid complex (D). Scale bar: 10 μm.

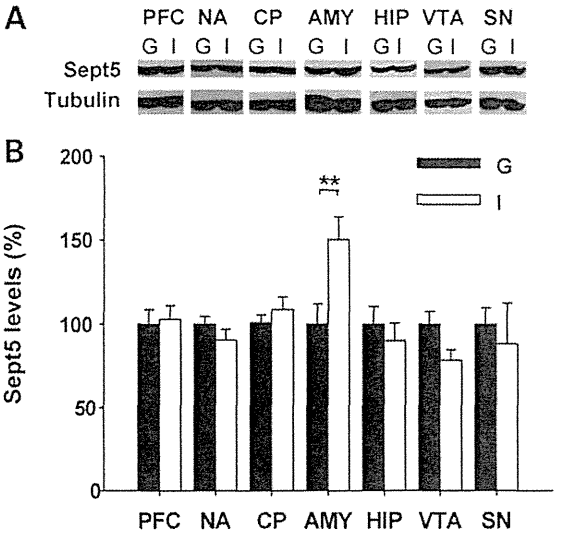

Figure 6. Effects of post-weaning housing conditions on Sept5 protein levels in the brain of C57BL/6J mice. Western blot analysis of Sept5 protein is shown. (**A**) Representative blots are shown for each region. (**B**) Quantitative analysis of Sept5 levels. Data are presented as means ± SEM. Although the overall housing effect was not significant ($F_{1,26} = 0.93$, $P = 0.3438$), there was a significant interaction between housing and the brain region ($F_{6,156} = 5.26$, $P < 0.0001$). This interaction was due to a significantly higher level of Sept5 in the amygdala of individually housed mice, as determined by *post hoc* comparisons (**significant at the 1% level). G, $n = 7–14$ mice for each region; I, $n = 8–10$ mice for each region. A sample from each mouse was used up to two to three times for all regions except for the SN and VTA; samples from the SN and VTA were used only once for each mouse. G, group housing; I, individual housing. PFC, prefrontal cortex; NA, nucleus accumbens; CP, caudate-putamen; AMY, amygdala; HIP, hippocampus; VTA, ventral tegmental area; SN, substantia nigra.

there was a statistically non-significant trend of 'positive' correlation in time spent in active social interaction at the second session between the two groups ($r^2 = 0.330$). Another possibility is that the Sept5 amygdala group had a heightened level of anxiety during the first session and exhibited a higher level of social interaction when anxiety presumably subsided by the second session. Although we did not see any phenotypic difference between the EGFP and Sept5 amygdala groups in anxiety-related traits in the elevated plus maze, anxiety seen in this task—where the source of anxiety is thought to originate from an open area and height—is not identical to what is expected in social interaction. Given that Sept5 elevations in these two limbic structures did not affect social interaction in the same way, more work is needed to identify the precise manner through which these structures mediate social behavior.

Post-weaning individual housing selectively raised Sept5 levels in the amygdala. This is consistent with our observation that Sept5 overexpression in the amygdala increases basal levels of affiliative social interaction. However, virally guided overexpression of Sept5 in the hippocampus also increased social interaction, but the housing condition did not induce a detectable increase in Sept5 levels in this structure. Our virally guided overexpression of Sept5 was confined to the dorsal hippocampus but was sufficient to raise levels of social interaction. As our hippocampal tissue for western blotting included the ventral and dorsal hippocampus and subiculum, it might not be sufficiently sensitive to detect highly local up-regulation of Sept5 within the hippocampus.

Although post-weaning individual housing and virally guided overexpression selectively increased Sept5 in the amygdala, these two treatments did not produce the identical behavioral effects. Moreover, constitutive *sept5* deficiency in KO mice and environmentally elevated Sept5 in the amygdala did not induce clear-cut opposing behavioral phenotypes. These results are hardly surprising, as constitutive *Sept5* deficiency and post-weaning individual housing are likely to induce many non-identical molecular alterations in the brain. In fact, this environmental manipulation, unlike selective overexpression of Sept5 in the amygdala, additionally induced many behavioral signs of reduced anxiety and stress. Notwithstanding these differences, Sept5 might be one of the converging points through which genetic deficiency and stress-related environmental factors impact social behaviors. One way to ameliorate social interaction deficits in 22q11.2 hemizygous patients could be to elevate the expression of Sept5 from the remaining copy of 22q11.2 by reducing stress levels.

The hippocampus is structurally altered in both ASD (58,59) and 22q11.2 hemizygous patients (60). The amygdala has been implicated as a site whose activity alteration is associated with defective social cognition in individuals with ASD and schizophrenia (61) and with 22q11.2 hemizygous deletions (62). While performing tasks that require social perception, altered activation patterns have been noted in the fusiform cortex and amygdala of individuals with 22q11.2 hemizygosity (62). A future challenge is to identify the precise network of structures through which Sept5 acts as a determinant for social cognition.

'Connectivity' is an emerging theoretical construct to explain diverse phenotypes seen in patients with schizophrenia

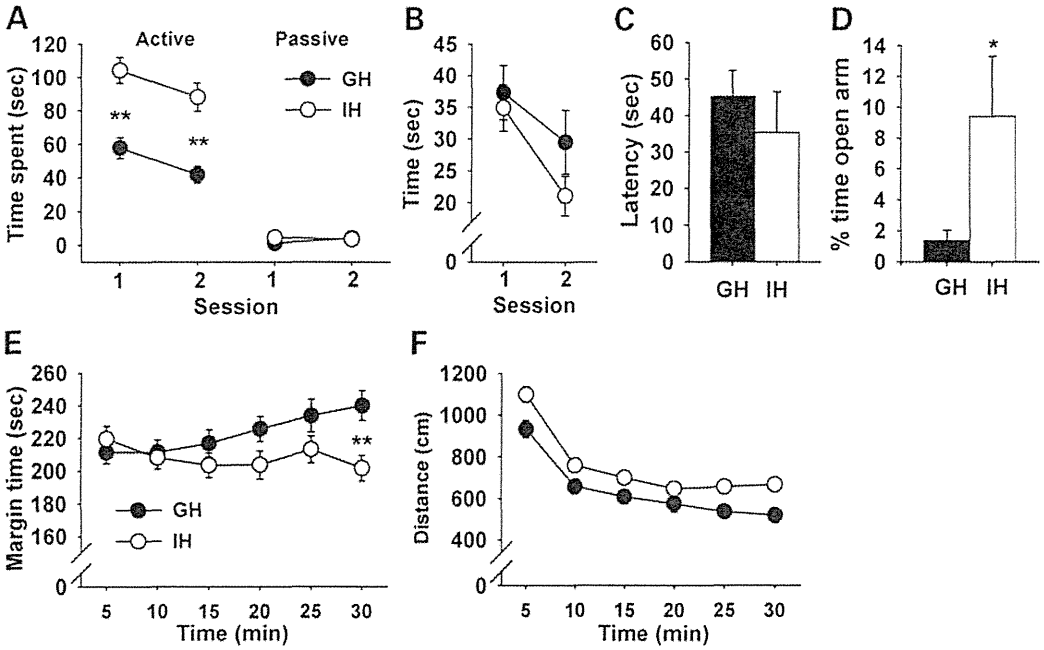

Figure 7. Behavioral effects of post-weaning housing conditions. Data are presented as means ± SEM. GH, group housing; IH, individual housing. (**A**) Active and passive social interactions. Main effects were significant for housing conditions ($F_{1,33} = 37.43$, $P < 0.0001$), social interaction type ($F_{1,33} = 248.27$, $P < 0.0001$) and session ($F_{1,33} = 8.24$, $P = 0.0071$). The only significant interaction was that between housing conditions and social interaction type ($F_{1,33} = 25.80$, $P < 0.0001$). Active social interaction was predominantly active affiliative social interaction in group-housed (98%) and individually housed (91%) mice. *Post hoc* comparisons indicated that individually housed mice spent more time in active social interaction than group-housed mice. Asterisks indicate statistically significant differences (1%) from GH mice as determined by the Newman–Keuls comparison. GH, $n = 18$; IH, $n = 17$. (**B**) Time spent contacting a novel object. Mice under the two housing conditions spent an indistinguishable amount of time interacting with a novel object, and equally habituated (housing, $F_{1,27} = 0.98$, $P = 0.3323$; session, $F_{1,27} = 30.18$, $P < 0.0001$; genotype × session, $F_{1,27} = 2.36$, $P = 0.136$). GH, $n = 15$; IH, $n = 14$. (**C**) Latency to find buried food. Mice under the two housing conditions were indistinguishable in the latency to find buried food ($t(13) = 0.72$, $P = 0.4873$). GH, $n = 7$; IH, $n = 8$. (**D**) The relative amounts of time spent in the open arms over both open and closed arms in the elevated plus maze. Individually housed mice spent more time in ($t(34) = 2.25$, $P = 0.0307$) and visited more frequently ($t(34) = 2.20$, $P = 0.0349$, not shown for clarity) the open arms than group-housed mice. GH, $n = 20$; IH, $n = 16$. (**E**) Thigmotaxis. Although there was no overall housing effect on the time spent in the margin ($F_{1,46} = 2.84$, $P = 0.099$) and neither group altered their time in the margin over time (time, $F_{5,230} = 1.96$, $P = 0.0862$), there was a significant interaction between the two factors ($F_{5,230} = 4.14$, $P = 0.0013$). This interaction was due to a significantly higher level of margin time in individually housed mice at the last time point. **Significant at the 1% level, as determined by Newman–Keuls *post hoc* comparisons. GH, $n = 25$; IH, $n = 23$. (**F**) Motor activity in an open field. Individually housed mice traveled more distance than group-housed mice, and both groups equally reduced their motor activity during the 30 min session (housing, $F_{1,46} = 8.86$, $P = 0.0046$; time, $F_{5,230} = 106.84$, $P < 0.0001$; housing × time, $F_{5,230} = 1.28$, $P = 0.2721$). GH, $n = 25$; IH, $n = 23$.

and ASD (63–65). Synaptic contact can be considered a structural basis of connectivity between neurons. Sept5-containing filaments, together with syntaxin-1A, are localized at pre-synaptic terminals, and Sept5 is thought to regulate neurotransmitter release at synapses together with the SNARE complex (66–68). Moreover, *in vitro* knockdown of *Sept5* has been shown to alter axon length and dendritic complexity (69,70). Proteins located at the trans-synaptic (i.e. neurexins) and post-synaptic (neuroligin and Shank3) sites are implicated in ASD- and schizophrenia-related phenotypes in other genetic mouse models (71). Our data add Sept5 as a pre-synaptic contributor to the synaptopathology of schizophrenia and ASD and support the notion that the symptomatic elements of schizophrenia and ASD stem from improperly formed or functioning synapses (71).

MATERIALS AND METHODS

Mice

Male C57BL/6J mice (Jackson Laboratories, Bar Harbor, ME, USA) and congenic *Sept5* KO and WT littermates were used. Congenic *Sept5* KO and WT mice were developed by backcrossing the original *Sept5* heterozygous mice (72) to C57BL/6J mice for 10 generations. Male *Sept5* WT, HT and KO littermates were housed together in cages (27 cm × 16 cm × 12.5 cm). Male C57BL/6J mice, housed in a group of three to four mice, were infused with an *EGFP* lentiviral vector or a *Sept5-EGFP* lentiviral vector (see Lentiviral vector and Surgery in what follows). Mice were given a week to recover before being tested. For the groups that were used to evaluate the impact of post-weaning housing conditions, 3-week-old male, C57BL/6J mice were randomly assigned to either group ($n = 3–4$) housing or individual housing and they were used for behavioral testing or killed for protein analysis after 6 weeks in these housing conditions. Mice remained in their housing condition until the end of testing. All mice were given access to food and water *ad libitum* and kept under a 14 h:10 h light/dark cycle, unless otherwise specified. Animal handling and use followed a protocol approved by the Animal Care and Use Committee of Albert Einstein College of Medicine, in accordance with National Institutes of Health guidelines.

Behavioral testing

Behavioral testing began at 2 months of age. This age point in mice represents the developmental phase after achieving sexual maturation around 1 month of age and before reaching mature adulthood at 3 months of age; many biological processes in the brain continue to change during this period (56,73). Mice were tested in a battery of assays based on our standard procedure (45,56,73–75).

Congenic *Sept5* mice and C57BL/6J mice were tested in the following order: social interaction, elevated plus maze and open field; two separate groups were tested either on novel object recognition or the buried food test. C57BL/6J mice were tested in the following order: social interaction, novel object recognition, open field, elevated plus maze and buried food test. A randomized order of assays is problematic, as a more stressful task affects performance on subsequent tasks (76). Therefore, tasks were given in order from less to more stressful, with a 1-day interval between tests so that repeated testing did not affect phenotypic expression. All testing was done during the light phase of the cycle. An hour before testing, mice were brought into a room outside the testing room. An observer was blinded to genotype and experimental groups.

Social interaction

We followed our protocol (45,56,73). Two mice were taken from their home cages and individually placed in new, separate cages for 30 min. Mice were next placed together in a new, third cage for two 5 min sessions separated by a 30 min interval: the second session evaluated recognition memory. Pairings were always made between a WT mouse and a KO mouse taken from different litters housed in different cages. For the viral overexpression experiment, group-housed, non-operated C57BL/6J mice were paired with *EGFP*- or *Sept5*-infused mice housed in different cages. For the housing experiment, group-housed C57BL/6J mice were paired with C57BL/6J mice that were individually or group-housed in different cages. Social behaviors were scored for active and passive behaviors by experimenters blinded to housing condition. Active behaviors included aggressive (i.e. tail rattle, bites, kicks, sideways offense, boxing, wrestling, mounting and pursuit) and affiliative (i.e. olfactory investigation and allogrooming) behaviors. Passive behaviors were escape, leap, side-by-side position and submissive posture. Time spent in aggressive, affiliative and passive interactions were analyzed separately.

Elevated plus maze

A mouse was placed on the central platform of the elevated plus maze facing one of the open arms. Behavior was recorded for 5 min. An observer blinded to the experimental condition rated the recordings. We analyzed the percentage of time spent in and of entrances to the open arms over the total time in and entrances to both the open and closed arms.

Locomotor activity

Four identical, automated open-field apparatuses (Truscan, Coulbourn Instruments, PA, USA) were used to measure spontaneous locomotor activity and thigmotaxis. Each 30 min session was analyzed in six 5 min bins. To assess horizontal locomotor activity and thigmotaxis, distance traveled (cm) in the entire open field (26 cm × 26 cm) and time spent (s) in the marginal area along the walls (a 4 cm band extending from the wall), respectively, were analyzed.

Novel object contact

At the beginning of testing, an individual mouse was placed in a new home cage for 30 min. The mouse was then moved into another home cage that contained a modified falcon tube (3 cm diameter × 8.5 cm length) during two 5 min sessions with a 30 min intersession interval. All activity was recorded by a digital camera placed above the home cage. An observer blinded to experimental condition scored the amount of time each mouse spent contacting the object. Sniffing and physical contact with the object were used for analysis.

Buried food test

For 2 consecutive days, a piece of the stimulus food (Honey Teddy Grahams, Nabisco, East Hanover, NJ, USA) was placed in their home cages in the presence of their normal mouse chow. On Day 3, normal chow was removed from the cage top and testing began 20–22 h later. A mouse was placed in a novel home cage containing 3 cm deep bedding (testing cage). After 5 min, the mouse was placed in another clean home cage. The stimulus food was buried about 1 cm beneath the 3 cm deep bedding in the test cage, and the mouse was then returned to the test cage. The latency to start consumption of the stimulus food was recorded. If the mouse did not find the stimulus food in 5 min, testing was terminated and that mouse received a latency of 300 s.

Lentiviral vector

The adult form of the mouse *Sept5_v1* gene (77) (RIKEN, Yokohama, Japan) was inserted into a lentiviral vector containing an internal ribosome entry site (*IRES*) and *EGFP*. *Sept5* was polymerase chain reaction (PCR)-amplified with primers with attB1/attB2 and introduced into a pDONR-221 vector by BP clonase reaction (Invitrogen, Grand Island, NY, USA). The IRES-EGFP sequence (Clontech, Mountain View, CA, USA) was amplified with primers with attB2/attB3 and introduced into a pDONR-P2R-P3 vector (Invitrogen) by BP reaction. The promoter region of calcium/calmodulin-dependent protein kinase II alpha (*CamkIIα*), a neuron-specific protein (78), was PCR-amplified with primers with attB4/attB1r and introduced into a pDONR-P4P1r vector (Invitrogen) by BP reaction. The *CamkIIα* promoter element, *Sept5*, and *IRES-EGFP* were introduced into a pLenti6.4/R4R2/V5-DEST vector (Invitrogen). A plasmid was generated by inserting $P_{CamkIIα}$-*Sept5-IRES-EGFP* or $P_{CamkIIα}$-*IRES-EGFP*. Using 293T cells transfected with the plasmid, we confirmed that Sept5 protein is expressed (Supplementary Material, Fig. S3A). Viral particles were generated by co-transfection of 293FT cells (Invitrogen) by the pLenti6.4/R4R2/V5-DEST-based plasmid-containing $P_{CamkIIα}$-*Sept5-IRES-EGFP* or $P_{CamkIIα}$-*IRES-EGFP* and three packaging helper plasmids, using the calcium phosphate method (79). Seventy-two hours after transfection, viral particles were collected and resuspended in phosphate-buffered saline. Viral titers were estimated by counting surviving cells following blasticidin.

Surgery

Male C57BL/6J mice were anesthetized with sodium pentobarbital [40 mg/kg, intraperitoneal (i.p.)] and were then placed in a stereotaxic apparatus (MyNeuroLab, Richmond, IL, USA). A 2.5 μl Hamilton syringe (Hamilton, Reno, NV, USA) with a 30-gauge needle was used to inject 0.3 μl of the *EGFP* lentiviral vector (2.30×10^6 TU/ml) or the *Sept5-EGFP* lentiviral vector (6.40×10^6 TU/ml) for a period of 5 min and the needle was left in place for another 5 min. Bilateral injections were made into the hippocampus (anterior-posterior (AP), −1.82 mm; medial-lateral (ML), 2.25 mm; dorsal-ventral (DV), 2.8 mm), amygdala (AP, −1.82 mm; ML, 3.0 mm; DV, 5.5 mm) or somatosensory cortex (AP, −1.82 mm; ML, 3.0 mm; DV, 2.0 mm). Mice were given a week to recover before being tested.

Immunohistochemistry

After behavioral analysis was completed, animals were anesthetized with sodium pentobarbital (62.5 mg/kg, i.p.) and perfused with saline followed by 4% paraformaldehyde. Brains were coronally sliced at 50 μm, covering the entire antero-posterior extent of the hippocampus and amygdala, and were examined for EGFP. A separate set of sections were immunohistochemically stained for NeuN (mouse anti-NeuN antibody, 1:200, Millipore) as a marker of neuron together with Texas-red-conjugated anti-mouse IgG (1:500, Jackson ImmunoResearch, West Grove, PA, USA) or Alexa594-conjugated anti-mouse IgG (1:500, Invitrogen) secondary antibody. Signals were analyzed under an epi-fluorescent microscope (Zeiss) and a confocal microscope (Leica).

To evaluate the extent of virally expressed Sept5, we used a small set of *Sept5* KO mice. KO mice received infusions of the *Sept5-EGFP* lentiviral vector into the hippocampus or basolateral amygdaloid complex and killed 1 week later. One set of sections were mounted and examined for EGFP. A separate set of adjacent sections were immunohistochemically stained with either a goat polyclonal Sept5 antibody (1:1000, Santa Cruz Biotechnology, Santa Cruz, CA, USA) or a mouse monoclonal Sept5 antibody (1:10 000, Assay Designs, Ann Arbor, MI, USA), following our standard Nickel-intensified DAB-staining procedure (80–82). EGFP and Sept5 signals were analyzed under an epi-fluorescent microscope (Zeiss) and a light microscope (Zeiss), respectively. The extents of EGFP and Sept5 protein signals overlapped (Supplementary Material, Fig. S2B–E), indicating that EGFP reliably represents the extent of virally expressed Sept5.

Western blot

Cervical dislocation was used to sacrifice mice for western blotting. The following brain areas were dissected out in saline on ice: prefrontal cortex, nucleus accumbens, caudate-putamen, amygdala, hippocampus, substantia nigra and VTA. Tissues were homogenized by sonication in electrophoretic mobility shift assay buffer. Sixty micrograms of sample, as determined by Bradford assay, was loaded into a 10% acrylamide gel. Transferred proteins on membranes were labeled with a goat polyclonal Sept5 antibody (1:200, Santa Cruz Biotechnology), followed by a donkey anti-goat horseradish peroxidase-conjugated IgG secondary antibody (1:5000, Santa Cruz Biotechnology). A rat monoclonal anti-tubulin antibody (1:5000, Abcam, Cambridge, MA, USA) was used in conjunction with goat anti-rat horseradish peroxidase-conjugated IgG secondary antibody (1:5000, Santa Cruz Biotechnology) to determine the amount of protein loaded. For the detection of Sept5 in 293T cells transfected with the plasmid, a mouse anti-Septin 5 (SP18) monoclonal antibody (1:200, Santa Cruz Biotechnology) and anti-mouse horseradish peroxidase-conjugated IgG secondary antibody (1:10 000, Vector) were used. Specific bands were visualized using SuperSignal West (Thermo Scientific, Waltham, MA, USA). Absorption was then measured using a GS-700 densitometer (Bio-Rad, Hercules, CA, USA) with the Quantity One software. The levels of Sept5 were normalized to tubulin and percentages of levels over standard housing were calculated for analysis.

Statistical analysis

All data are presented as the mean ± standard error of the mean (SEM). Statistical significance was determined by analysis of variance followed by Newman–Keuls *post hoc* comparisons. When two groups were compared, Student's *t*-test was used. The minimum level of significance was set at 5%.

SUPPLEMENTARY MATERIAL

Supplementary Material is available at *HMG* online.

ACKNOWLEDGEMENTS

We thank Dr Dan Scott for blinding experimental groups.

Conflict of Interest statement. None declared.

FUNDING

This work was supported by the National Institutes of Health (HD05311), National Alliance for Research on Schizophrenia and Depression Independent Investigator Award and the Maltz Foundation to N.H.

REFERENCES

1. Penn, D.L., Corrigan, P.W., Bentall, R.P., Racenstein, J.M. and Newman, L. (1997) Social cognition in schizophrenia. *Psychol. Bull.*, **121**, 114–132.
2. Sigman, M. (1998) The Emanuel Miller Memorial Lecture 1997. Change and continuity in the development of children with autism. *J. Child Psychol. Psychiatry*, **39**, 817–827.
3. Swillen, A., Devriendt, K., Legius, E., Eyskens, B., Dumoulin, M., Gewillig, M. and Fryns, J.P. (1997) Intelligence and psychosocial adjustment in velocardiofacial syndrome: a study of 37 children and adolescents with VCFS. *J. Med. Genet.*, **34**, 453–458.
4. Golding-Kushner, K.J., Weller, G. and Shprintzen, R.J. (1985) Velo-cardio-facial syndrome: language and psychological profiles. *J. Craniofac. Genet. Dev. Biol.*, **5**, 259–266.
5. Baker, K.D. and Skuse, D.H. (2005) Adolescents and young adults with 22q11 deletion syndrome: psychopathology in an at-risk group. *Br. J. Psychiatry*, **186**, 115–120.